Universidad Zaragoza
1542

FINAL MASTER PROJECT

Concerned nanotechnology: Screen printed electrodes (SPE) to detect nanoparticles in natural media.

Author
Walvin Ramiro Córdova Vera

Supervisor
Dr. Juan Carlos Vidal

NANOSTRUCTURED MATERIALS FOR NANOTECHNOLOGY APPLICATIONS
Institute of Nanoscience of Aragón / Science Faculty
University of Zaragoza
2013-2014

This is to certify that

D. Walvin Ramiro Córdova has developed a personal work corresponding to the proposal "*Concerned nanotechnology: Screen printed electrodes (SPE) to detect nanoparticles in natural media*" whose final report is presented here as Final Master Project of the "Máster Universitario en Materiales Nanoestructurados para Aplicaciones Nanotecnológicas" This work has been developed in the labs of the "Grupo de Espectroscopía Analíca y Sensores (GEAS)", IUCA under my supervision

Zaragoza, September 4th, 2014

Dr. Juan Carlos Vidal Ibáñez

This work has been supported by a Spanish competitive project CTQ 2012-38091.

Acknowledgements

Special thanks to the "***Instituto Universitario de Investigación en Ciencias Ambientales de Aragón, IUCA***" by the scholarship "*Apoyo a la Investigación*" awarded for the current academic year and also for allowing me to realize my final master project in its facilities. I also want to thank the research group "Grupo de Espectroscopia Analítica y Sensores" to allow me to work with them in its laboratories and with its equipments, as well as the "Departamento de Química Analítica" for its support.

Thank my tutor, Dr. Juan Carlos Vidal for collaboration and guidance provided in the development of this project. I also want to thank Dra. Gemma Cepriá Pamplona for her assistance in these difficult times.

Thanks to Dr Mario Pérez Riera and Dr Francisco José Ruíz Blasco of the "Departamento de Matemáticas, Área de Análisis Matemático" who had helped me with Fourier transform smoothing of the chronoamperograms, without their help no collision events could have been ever seen in our lab.

Many thanks to my colleagues in laboratory for their patience and support, special thanks to Dr. Laura Sanchez for allow me use their STEM data.

TABLE OF CONTENTS

1. ABBREVIATIONS

AA	Ascorbic Acid
AE	Auxiliary Electrode
AFM	Atomic Force Microscopy
AP10	Argentum Plus 10ppm
AP25	Argentum Plus 25ppm
DLS	Dynamic Light Scattering
FFF	Field-Flow Fractionation
GC	Glassy Carbon
GC-ME	Glassy Carbon Microelectrode
HRTEM	High Resolution Transmission Electron Microscopy
ICP-MS	Inductively Coupled Plasma Mass Spectrometry
ME	Microelectrode
NPs	Nanoparticles
PC	Particle Collision
PCS	Photon Correlation Spectroscopy
PEN	Project on Emerging Nanotechnology
PFM	Peak Fitting Module
Pt-ME	Platinum Microelectrode
RE	Reference Electrode
ROS	Reactive Oxygen Species
SD	Standard deviation
SEM	Scanning Electron Microscopy
SN30	Source Naturals 30ppm
SOD	Superoxide Dismutase Activity
SPCE	Screen Printed Carbon Electrode
TEM	Transmission Electron Microscopy
VIP	Voltammetry Immobilized Particles
WE	Working Electrode
XPS	X-ray Photoelectron Spectroscopy

2. SUMMARY

Nanomaterials have entered strongly in our society because they provide clear advantages. The consequences of its use, interactions with environment and regulations are growing fields of research.

This final Master project is focused on the use of electroanalytical techniques for the characterization of nanostructured materials, focusing specifically on the nanoparticles.

The project can be divided in two parts:

1.- Linear voltammetry combined with electrochemical cell and/or screen printed electrodes is used for the characterization of silver nanoparticles in real samples deposited on the working electrode (*Voltammetry Immobilized Particles, VIP)*. Real samples are solutions used as dietary supplements. The study is based on the total oxidation of the nanoparticles and the relationship between the peak position observed in the voltammogram and the nanoparticle size. This technique was applied to real samples to detect aggregation of the nanoparticles and check the influence of the electrode on this phenomenon.

2.- Chronoamperometry combined with microelectrodes is used for the characterization of silver nanoparticles and cerium oxide nanoparticles in suspension (*Particle Collision, PC)*. Charge exchange is produced at the surface of the electrode when a nanoparticle hits the electrode. The amount of charge involved depends on the size of the nanoparticles following a mathematical equation. Different procedures have been used for each type of nanoparticle. The study was carried out on standards and samples in the case of silver and only on standards in case of cerium oxide. The results give the size distribution for each type or sample of nanoparticle.

3. INTRODUCTION

Nanotechnology is consolidating as the new era of the materials. On the history of materials and progress with humanity, we can talk about of Stone Age, Bronze Age, Iron Age and the Information age in the second half of the 19th century. In the last ten or twenty years have seen enormous progress in the research, production and adaptation of nanotechnology. That is why it is already considered as the next era of the materials. The progress made in the field of nanotechnology has resulted in several products that are already commercial. The applications are varied and some examples are described below (**Figure 1**):

A. Use of Zinc oxide and/or Titanium dioxide nanoparticles in sunscreens.[1]
B. Use of Silver nanoparticles for its antibacterial properties in detergents, clothing, keyboards, pacifiers, etc.[2]
C. Use of carbon nanotubes composite to improve the hardness and strength in sports equipment like tennis racket or bicycles.[3]
D. Use of cerium oxide nanoparticles as an additive in diesel motor vehicles.[4]

Figure 1. Figure shows some nanotechnology products.

There are many more examples with real application of nanotechnology and the previous ones are just a small sample. The plan called, Project on Emerging Nanotechnologies (PEN), shows different products that contain nanotechnology, advances, potential risks and information of benefits to be gained.[5]

The advantages of nanotechnology are clear and therefore the production in this field is increasing and will increase in the future. Lux Research, independent research and advisory firm on emerging technologies, estimates that nanotechnology will impact more than over $2.5 trillion worth of manufactured goods by 2015. In **Figure 2** are collected some estimations about projections of revenues on nanotech-enabled products until 2015.[6]

Figure 2. Figure shows the forecasts of benefits stipulated until 2015. *(Extracted from reference [6])*

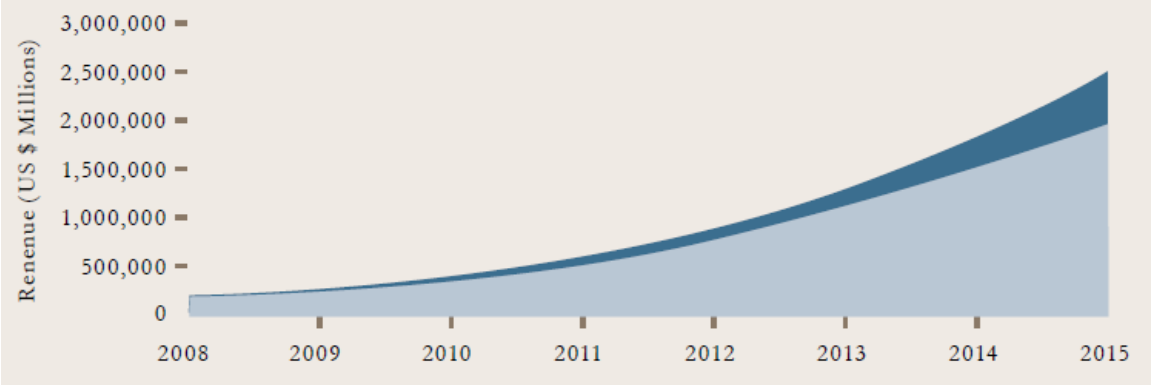

Given the above and the undeniable presence of nanotechnology in our future, we must know how this new technology will interact with living things and their environment.

For this reason, some questions arise that need to be answered as: we should be afraid of nanotechnology?, Should nanoproducts be labeled?, Is the use of nanomaterials in food safe?, Do nanoproducts require special disposal?. All these questions are mainly related to the nanomaterials life cycle, their interaction with the environment and subsequent treatment.

The present final Master project is focused to try to clarify the answers to the above questions. This work is centered on metal nanoparticles, in particular, silver nanoparticles (AgNPs) and cerium oxide nanoparticles (CeO_2NPs or nanoceria).

The next and final part of introduction describes some important points about these nanoparticles as potential uses, how they work, toxicity, techniques of identification and/or quantification, etc.

3.1. SILVER NANOPARTICLES (AgNPs)

Among various anti-microbial agents, silver has been most studied and used to fight against infections and prevent spoilage for many centuries.[7] The principal use of AgNPs is like an antibacterial agent. AgNPs have been shown to be effective biocide against bacteria such as *Escherichia coli*, *Staphylococcus aureus*, *Staphylococcus epidermis*, *Leuconostoc mesenteroides*, *Bacillus subtilis*, *Klebsiella mobilis*, and *Klebsiella pneumonia* among others. Also they can effective against some fungi (*Aspergillus niger*, *Candida albicans*, *Saccharomyces cerevisia*, *Trichophyton mentagrophytes* and *Penicillium citrinum*) and even virus (Hepatitis B, HIV-1, syncytial virus)[2]

There are many methods to produce AgNPs such as: chemical reduction process and photo-catalytic, reverse micelle based methods and even biological synthesized and others.[7] However, the most common method is the chemical reduction of silver salts.

A major advantage of using nanoparticles is that the surface/volume ratio is much higher, and therefore, for the same volume the surface increases and the anti-bacterial effects can be maximized.

The antibacterial effect of AgNPs is mainly produced by the silver ions (Ag(I)). This effect of AgNPs can be explained as: (i) release of silver ions and generation of reactive oxygen species (ROS) in the surroundings of the bacteria; (ii) interact with membrane proteins affecting their correct function and inhibits the growth of bacteria; (iii) accumulate in the cell membrane affecting membrane permeability; and (iv) enter into the cell where it can generate ROS, release silver ions, and affect DNA. **Figure 3** is a diagram that summarizes the interaction between the particles and bacteria.[2,6]

Figure 3. Diagram summarizing the interaction between AgNPs and bacteria. *(Extracted from reference [2])*

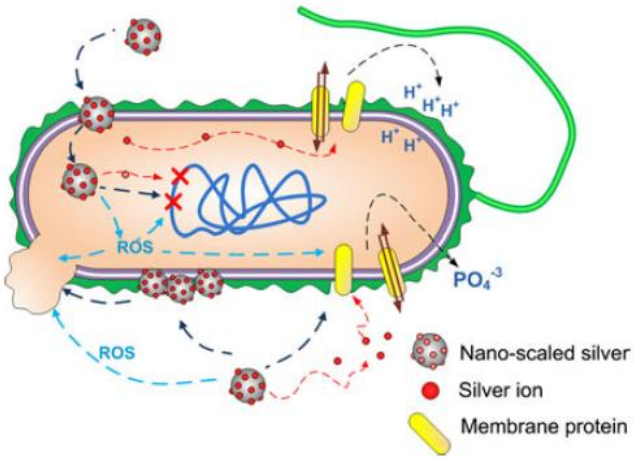

Antibacterial property of AgNPs is affected by the particle properties such as size, shape, coating, surface charge, etc. because the mechanism of Ag(I) release depends on them. For example, AgNPs of smaller size may exert higher toxicity due to their higher specific surface area and associated faster Ag(I) release rate compared to larger AgNPs.[9]

Researchers have also found evidence of toxicity for mammalian cells. Among the affected species we can mention zebrafish, fruit fly, mices, rats and also humans. **Table 1** shows some examples of mammalian cell affected by the toxicity of AgNPs.[2]

Table 1. Evidence of AgNPs toxicity for mammalian cells. *(Extracted from reference [2])*

Target cell/organism	Key aspects
Rat lung cells	Reduction in lung function and inflammatory lesions
Sprague-Dawley rats	Silver nanoparticles accumulation in olfactory bulb and subsequent translocation to the brain
Mouse stem cells	Cell leakage and reduction of mitochondrial function
Rat liver cells	Cell leakage and reduction of mitochondrial function
Human fibrosarcoma and human skin/carcinoma	Oxidative stress. Low doses produced apoptosis and higher dose necrosis
Mouse fibroblast	50 μg/mL induced apoptosis to 43.4% of cells
Human colon cancer	100 μg/mL produced necrosis to 40.2% of cells
Human glioblastoma	Silver nanoparticles were found cytotoxic, genotoxic and antiproliferative
Human fibroblast	Silver nanoparticles were found cytotoxic, genotoxic and antiproliferative

The field of science which aims to standardize physical measurements at the nanometer scale is called *nanometrology*.[8] The characterization and quantification of nanoparticles is a difficult analytical process due to its high dependence on particle size and nature, concentration in the sample, physico-chemical characteristics of the solution and fundamental principles of analytic technique. The most common techniques used for size characterization include laser techniques, such as photon correlation spectroscopy (PCS), electron microscopes (scanning electron microscopy, SEM, transmission electron microscopy, TEM), also atomic force microscopy (AFM) and size separation techniques (field-flow fractionation, FFF, hydrodynamic chromatography and size-exclusion chromatography).[10]

3.2. CERIUM OXIDE NANOPARTICLES (CeO_2NPs or nanoceria)

In contrast to the silver, cerium chemistry is not yet fully known and need to know more about their chemical reactivity.

Cerium is a rare earth element which can form two main crystal structure, cerium(IV) oxide (CeO_2) and cerium(III) oxide (Ce_2O_3). The most important for their applications is CeO_2 nanoparticles or nanoceria. Today, nanoceria is being used in a variety of fields such as an active catalyst in vehicle emission system for oxidation of pollutant gases[11], in biomedicine as an antioxidant in treatments produced by ROS, also are used as an electrolyte material for solid oxide and proton exchange membrane fuel cells among others.

Potential use of nanoceria is due to its crystal structure. CeO_2 is not a stequiometric compound because the outermost layers of the nanoparticle have some defects. These defects are responsible that the most external atoms to be less coordinated that internal. To compensate these defects, the oxygen is released reversibly and produces the reduction of the oxidation state of some atoms of Ce(IV) to Ce(III). This facility to change the oxidation state from Ce(IV) to Ce(III) and vice versa as a function of environmental requirements is responsible for the reactivity of nanoceria. The inner core of the nanoparticle has an almost perfect crystal structure of CeO_2 where all spaces are occupied by oxygen and cerium. As mention above, the most external layers of particles are responsible for the reactivity. If nanoceria are smaller, the reactivity will be higher because the size reduction involves an increase in the number of external vacancies relative to total atoms. **Figure 4** shows the cubic structure of CeO_2.[12]

Figure 4. Typical cubic structure of CeO_2 (Red spheres: Oxygen atoms; Cream spheres: Cerium atoms). *(Extracted from reference [12])*

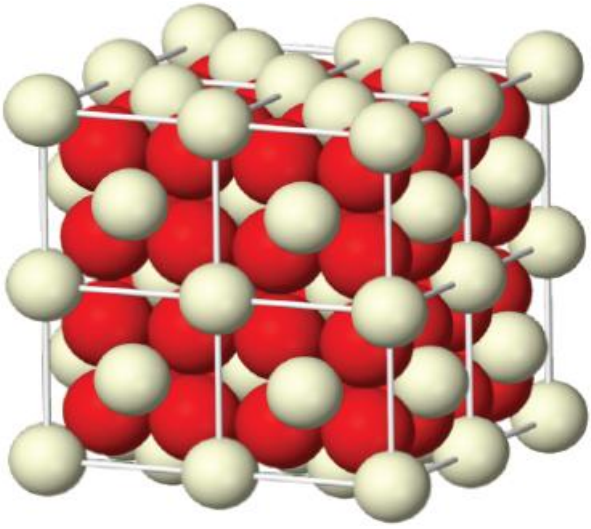

Nanoceria acts as a catalytic antioxidant in biological model systems. These nanoparticles show two mimetic activity, superoxide dismutase activity (SOD) to convert superoxide anion to hydrogen peroxide and catalase mimetic activity to convert hydrogen peroxide into water and molecular oxygen. These two mimetic activities are highly dependent on the Ce(III)/Ce(IV) ratio, so SOD activity is less efficient with high concentrations of Ce(IV) and catalase activity is more efficient with low levels of Ce(III).[13-15] Furthermore, these nanoparticles are able to recover its catalytic activity and therefore may have pseudoinfinite half-life.[13, 16]

The most common synthesis method is oxidation at room temperature of salts of Ce(III), $Ce(NO_3)_3$ for example, by adding strong bases or ammonium salts. In any case it is an alkaline-based precipitation of Ce(III).[12]

The main techniques for the characterization of nanoceria are electronic microscopy techniques (TEM and HRTEM), X-ray photoelectron spectroscopy (XPS), Raman, Inductively coupled plasma mass spectrometry (ICP-MS), UV spectroscopy, dynamic light scattering (DLS) and zeta potential.[12,13,16]

Regarding the toxicological risk of nanoceria, we can mention that these nanoparticles can acts as a producer of ROS or as an antioxidant, antagonistic effects. The behavior depends on the organism, environment, dose and physical characteristics of nanoceria, for example:

- In a study of two photosynthetic organisms, cyanobacteria and green algae, was found that nanoceria significantly inhibits photosynthesis in cyanobacteria, while having a dual effect on green algae because it produces a slight stimulation of growth at low concentrations and strong inhibition at high concentrations.[17]
- In another example, the dose and time of exposure to nanoparticles is studied on human lens epithelial cells. The results show that 100µg/mL is acceptable for an exposure time of 48h. However, exposure time plays a more important role that the concentration indicating a potential genotoxicity for higher exposures.[18]

Finally, the following table (**Table 2**) shows some effects, beneficial and adverse, of exposure to nanoceria[19]

Table 2. Reports of nanoceria effects. *(Extracted from reference [19])*

Reports of ceria ENM effects

Study subject	Ceria ENM size (nm)	Ceria ENM concentration (nM)	Effect
***In vitro* studies reporting beneficial effects of ceria ENMs**			
Hemoglobin	3 to 8	50,000 to 1,000,000	Scavenging
MCF-7 breast tumor and CCL-135 normal lung fibroblast cells	3 to 5	10	Protection
CRL 1541 normal human colon cell	3 to 5	1 to 100	Protection
HT-1080 human breast fibrosarcoma cells	16	1 to 10, but not 100	Protection
Mouse-derived cardiac progenitor cells	5 to 8	59,000 to 290,000	Protection
J774A.1 mouse macrophages	3 to 5	10,000	Reduction
Rat heart-derived embryonic myocytes		10	Inhibition
A549 human basal epithelial adenocarcinoma cells	30, 50 and 300	29,400 to 235,000	Increased viability, decreased oxidation, not size or dose dependent
A549 cells	20	20,000 to 140,000	Decreased viability via oxidative stress
HT22 hippocampus derived cells	6 and 12	1 to 120,000; ≥~0	Enhanced cell survival
SH-Sy5Y neuroblastoma cells	6 to 16	600,000	Reversal
Rat spinal cord neurons	3 to 5	10	Enhanced viability
Mixed culture of rat cortical neurons and glial cells	7, 10, and 50	10	Protection
Mouse hippocampal slices	Not reported	600 to 5000	Protection
***In vitro* studies reporting adverse effects of ceria ENMs**			
3T3 rodent fibroblast and MSTO-211H human mesothelioma cells	19	20,000 to 90,000 for 6 days or 40,000 to 170,000 for 3 days	Decreased viability and DNA content
BEAS-2 human bronchial epithelial cells	15 to 45	6000 to 230,000	Decreased viability, death, and induction of oxidative stress-related genes
***In vivo* studies reporting beneficial effects of ceria ENMs**			
Rats	3 to 5	1 to 20 nmol injected into rat vitreous humor	
Knockout mice that develop intra-retinal and sub-retinal neovascular lesions	3 to 5	172 nmol bilateral intraocular injection post-natal day 7 172 nmol bilateral intraocular injection post-natal day 28	Inhibited ROS production and lesion formation Reduced lesions
Mouse model of retinal degeneration	Not reported	20 nmol into the heart post-natal days 10, 20, and 30	Decreased retinal ROS
Rats	25	0.0001 nmol/kg on days 1, 3, 5 and 7	Protection
Athymic nude mice	3 to 5	0.06 nmol/kg thrice weekly ip for 2 weeks	Reduction
5 week old transgenic mouse model of cardiomyopathy	7	~300 nmol/kg twice weekly iv for 2 weeks	Partially converted cardiac function to control levels
***In vivo* studies reporting adverse effects of ceria ENMs**			
Mice	~130	290,000 to 2,325,000 nmol/kg intratracheal instillation	Neutrophil elevation and inflammatory cytokines in the bronchoalveolar fluid, lung granulomas 7 and 14 days later
Rats	15 to 30	641 mg/m^3 inhalation for 4 h	Increased oxidative stress 1, 2 and 14 days later
Rats	30	290,000 to 4,350,000 nmol/kg iv	Kupffer cell activation and brain oxidative stress
Rats	5	495,000 nmol/kg iv	Oxidative stress in the brain 30 days later
Rats	5	495,000 nmol/kg iv	Hepatic granuloma, apoptosis and oxidative stress 30 days later
Rats	30	495,000 nmol/kg iv	Hepatic granuloma 30 and 90 days later, oxidative stress in liver and spleen

4. OBJECTIVES

GENERAL OBJECTIVES

- The student should develop the ability to work in a research project that requires the use of many different equipment and technologies in a responsible way and never forget he is not alone and the meaning of working within a team.
- He should be able to recognize his deficiencies and consequently he should find the way to acquire the knowledge he lacks.
- The student will be aware of the necessity of being responsible about what it is done in the laboratory and how much it can affect life and environment.

PARTICULAR OBJECTIVES

- Full literature reviewing to know the state of the art of the subject.
- Adequate manipulation of the instrumentation required for the research project.
- Developing an analytical procedure that enables the size determination of nanoparticles in a suspension.
- Mathematical treatment of the data to obtain the pursued information: FFT filtering of the signal, deconvolution algorithms, peaks adjustment procedures.
- Interpretation of the data to explain the phenomena that can be observed in suspension and on the electrode surface.

5. VOLTAMMETRY OF IMMOBILIZED PARTICLES (VIP)

5.1. INTRODUCTION

Voltammetry of immobilized particles (VIP) was studied and developed in the 90s by Prof. Scholz.[20-22] It is based on a simple technique of immobilization of solid particles and liquid droplets on the electrodes.[23] Then the drop is dried and voltammetry was performed in the appropriate electrolyte.

There are theoretical and experimental articles that deal with VIP.[24-26] The radius of nanoparticles could be obtained by VIP experiments because there is a relationship between size and peak potential. This is related with the characteristic Gibbs free surface energy of nanoparticles which differs from energy for macroobjects. So, the standard electrode potential (E^0_{np}) is lower than the redox standard potential for bulk metal (E^0_{bulk}) and the following equation was used by Redmond et. al. to describe this phenomena.[24]

$$E^0_{np} = E^0_{bulk} - \frac{(2\gamma v_M)}{zFr} \quad \begin{cases} \gamma: surface\ tension \\ v_M: molar\ volume \\ z: lowest\ valence\ state \\ F: Faraday's\ constant \\ r: radius \end{cases}$$

Another study reveals that the degree of dispersion of the sample affects the shape of the voltammograms. So, if we have small nanoparticles and more dispersion, the range of oxidation potentials increases.[25] Therefore, we can use the electrochemical data to assess the degree of dispersion of nanoparticles assemblies and the average particle radius. Indeed, our research group has conducted a previous study of AgNPs using VIP[27] which will be used later. The paper of this work is found in the final annexes. (annex **A0**)

5.2. MATERIALS

Three different samples were purchased from specialized health care shops. The names of them are collected in **Table 3**.

Table 3. Names, concentration and abbreviations of the samples used in this work

Name	Concentration	Abbreviation
Source Naturals	30ppm	SN30
Argentum Plus	10ppm	AP10
Argentum Plus	25ppm	AP25

In some experimental processes, some salts as KCl, $KClO_4$ and $FeCl_3$ were necessary. In addition, the polymer Nafion was necessary to modification of SPCE.

All solutions and dilutions of AgNPs were prepared with ultrapure water (Mili-Q Advantage). These last are stored in the dark to avoid the oxidation of nanoparticles. Each nanoparticle solution was sonicated in ultrasonic bath for just one minute before their use.

Voltammetric measurements were carried out with Autolab PGSTAT-12 potentiostat (Utrecht, The Netherlands) controlled by computer.

Two different approaches have been used. The different electrodes used are detailed in the following lines and a general scheme is included in **Figure 5**:

1. 20mL voltammetric cell with Ag/AgCl/3M NaCl reference electrode, Pt wire auxiliary electrode and glassy carbon (GC) working electrode with 3mm of diameter.
2. Screen Printed Carbon Electrode (SPCEs) with working and auxiliary electrodes printed from carbon-based ink (Gwent) and the pseudoreference electrode based on silver ink. The diameter of working electrode is 4mm.

Figure 5. The figure shows a diagram of the two approaches used in this section.

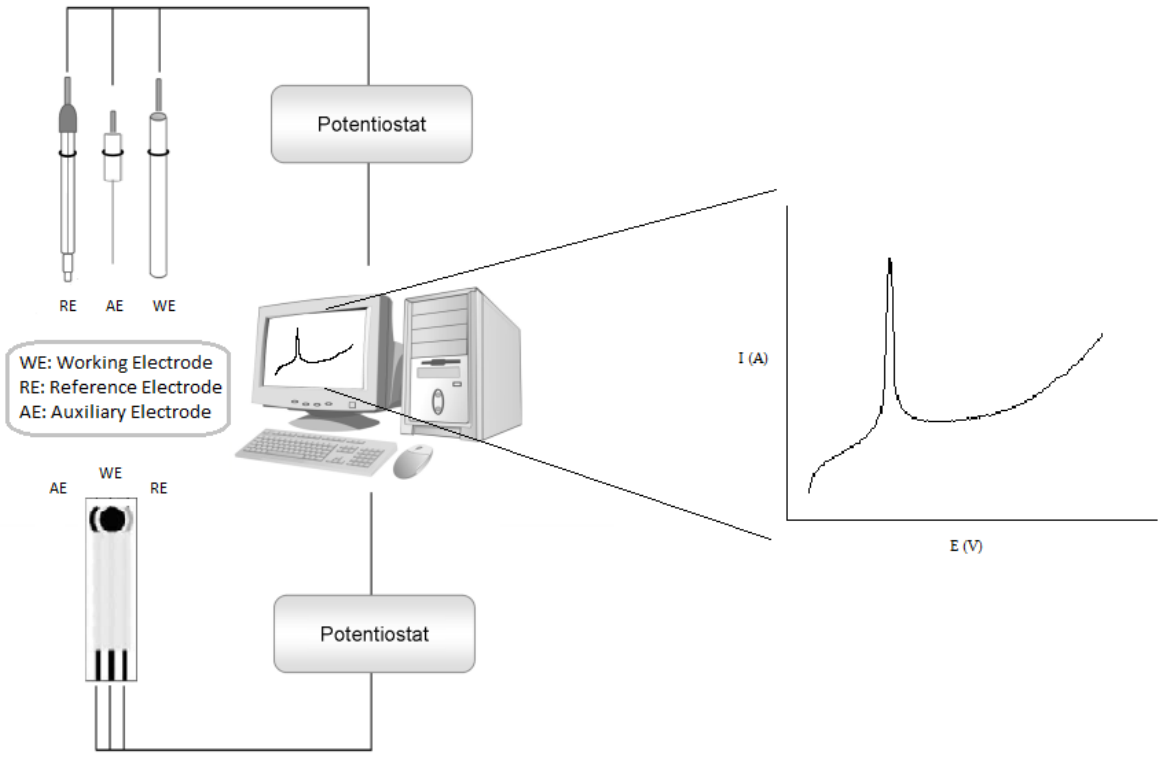

5.3. PROCEDURE

5.3.1. Samples of AgNPs on Glassy Carbon electrode (GC)

The sample AP25 was diluted twice, SN30 was diluted five times and AP10 was used without dilution.

The sample or its dilution is sonicated for 1 minute. Then 3µL of sample were drop cast on the graphite disk of the GC electrode. The solution should not reach the polymeric substrate. Then the drop was dried under nitrogen flow avoiding its displacement and the loss of material and aggregation. 10mL of 0.1M $KClO_4$ was used as the supporting electrolyte in the electrochemical cell. When the drop is dried, the electrodes are introduced into the electrochemical cell and start to measure the voltammograms. The working electrode is withdrawn from the cell and washed twice with mili-Q water. Then it can be air dried, or with nitrogen flow to accelerate the drying process, and then the process is repeated. The electrochemical measurements were performed in triplicate for each sample.

Measurement parameters: Linear sweep voltammetry was used in all measures with the following parameters:

Begin potential (V)	0.0
End potential (V)	0.8
Step potential (V)	0.00412
Scan rate (V/s)	0.02

5.3.2. Samples of AgNPs on a modified SPCE.

All samples were diluted to 1ppm. As in the previous case, the solutions are sonicated for 1 minute just prior to their use; in any case, they are stored in the dark.

We need stable and reproducible measurements to relate the peak potential with a certain diameter. The pseudoreference electrode (RE), based on Ag ink, is not very stable. Therefore, its modification is required to obtain useful measurements of peak potential. 3µL of 1M $FeCl_3$ was deposited over the RE for 1 minute to form a layer of AgCl. The excess of $FeCl_3$ was washed with mili-Q water and air dried. Finally, 3µL of 5% Nafion in ethanol saturated with KCl were deposited on the modified RE and allowed to dry at room temperature.[27] At the end, the modified RE is composed by layers of Ag/AgCl/KCl.

For sample measurements, 3µL of each sample are deposited on the working electrode of the modified SPCE. The drop is dried under nitrogen flow and then 70µL of 0.1M

$KClO_4$ was used as electrolyte to cover all three electrodes. At this point we can obtain the voltammograms. The same modified SPCE was washed twice with mili-Q water and dried in a nitrogen flow. Then, the process is repeated because the modification of the SPCE improves the reproducibility and robustness. The electrochemical measurements were performed in triplicate for each sample.

Measurement parameters: Linear sweep voltammetry was used in all measures with the following parameters:

Begin potential (V)	-1.5
End potential (V)	0.4
Step potential (V)	0.00412
Scan rate (V/s)	0.02

Measurement parameters are different that in the previous approach because the electrode system is different.

5.4. CALCULATION

In order to obtain the diameter in the samples, we use the calibration curves of our previous work cited on reference [27]. As we mentioned in the paper, we have two calibration plots for the GC electrode and two more for the modified SPCE.

The sample peaks are analyzed to obtain the peaks of the possible aggregations of AgNPs. This procedure has been performed by deconvolution of peaks in Origin 7.0 software with Peak Fitting Module (PFM). The results sheet released gives a wide variety of data; but we only use the *"CenterMax"* which is the peak potential (E_p). This peak potential is used to obtain the diameters. Then the mean diameter is obtained from the two calibration curves, and finally the generated values are averaged to obtain the final result. The procedure is repeated for each sample in the two approaches, GC and SPCE.

5.4.1. Samples of AgNPs on Glassy Carbon electrode (GC)

AgNPs standards with different diameters (10nm, 20nm, 40nm, 60nm and 100nm) were used to obtain the following calibration curves. The concentration for all standards was 0.5ppm.

The calibration curves are:

$$\text{First calibration curve:} \quad E_p = 0.168 + 0.054(\text{LogD})$$
$$\text{Second calibration curve:} \quad E_p = 0.174 + 0.066(\text{LogD})$$

In all instances, the regression coefficient was greater than 0.99

5.4.2. Samples of AgNPs on a modified SPCE.

The way to obtain calibration curves has been described above, standards with different diameters and 0.5ppm in concentration.

The calibration curves on modified SPCE are:

First calibration curve: $E_p = -0.151 + 0.217(\mathrm{LogD})$

Second calibration curve: $E_p = -0.113 + 0.1002(\mathrm{LogD})$

In all instances, the regression coefficient was greater than 0.99

5.5. RESULTS

5.5.1. Samples of AgNPs on Glassy Carbon electrode (GC)

Figure 6 shows two examples of each sample voltammogram that underwent deconvolution. All voltammograms of the samples are collected in the annex **A1**.

Figure 6. Figure collects two examples of each sample measured on GC that underwent deconvolution. (A and B) AP10, (C and D) AP25 and (E and F) SN30.

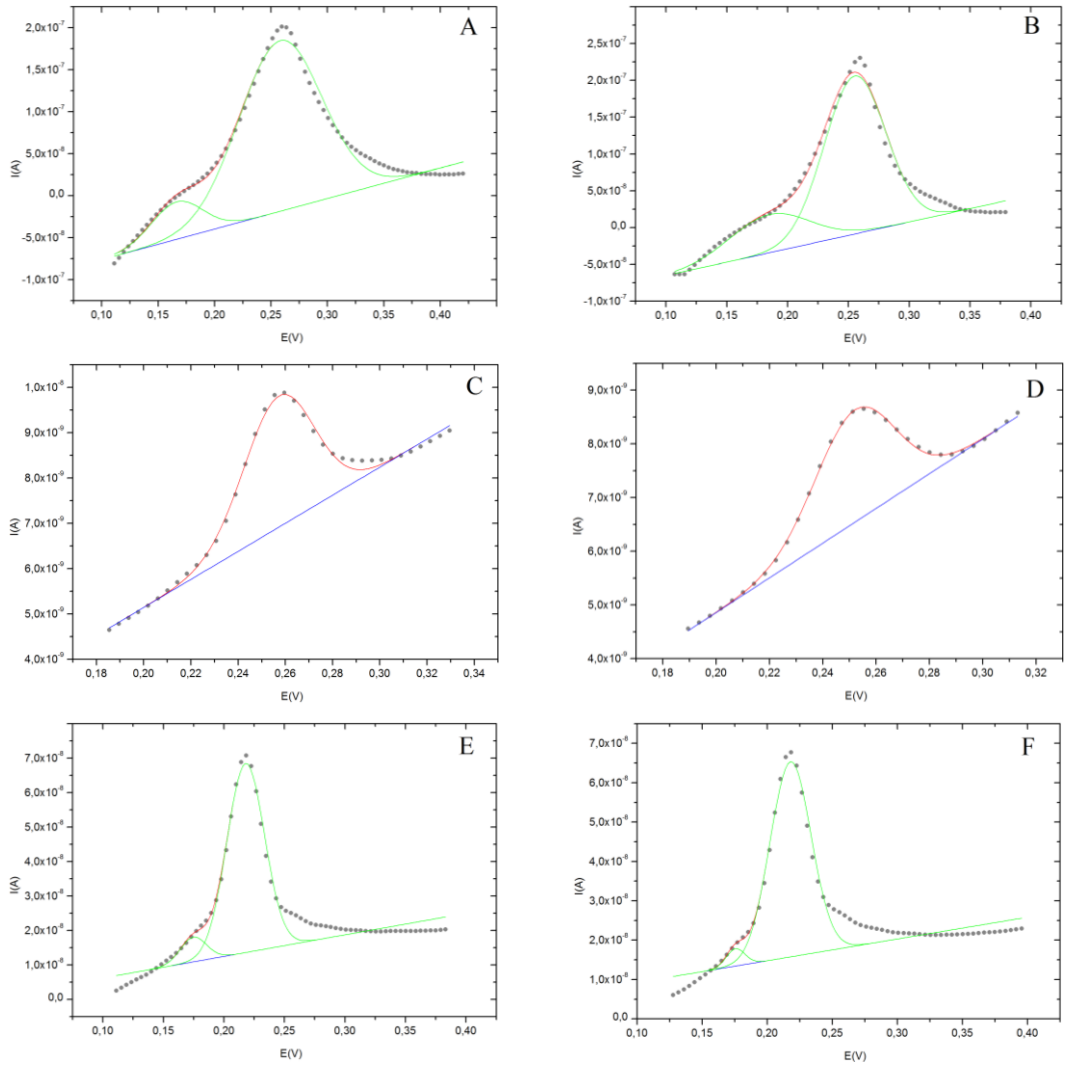

In the **Table 4** are collected the results of the samples subjected to deconvolution and the diameters obtained by the calibration. The inaccuracy of the results is presented by the standard deviation (SD).

Table 4. The table summarizes the average diameter and standard deviation of the sample peaks on GC after deconvolution. Each value is the average of three different mean values generated after interpolation in the two respective calibration curves. *The diameters extracted from reference [27] are also shown.

Samples	Peaks	Diam. (nm) ± SD	*Diam. (nm) ± SD
AP10	1^{st} peak	1 ± 1	45 ± 15
	2^{nd} peak	30 ± 3	
AP25	1^{st} peak	25 ± 7	14 ± 2
SN30	1^{st} peak	1 ± 0	20 ± 2
	2^{nd} peak	7 ± 1	

5.5.2. Samples of AgNPs on a modified SPCE.

As in the previous case, in the **Figure 7** two examples of each sample are shown. All voltammograms of the samples are collected in the annex **A2**.

Figure 7. Figure collects two examples of each sample measured on modified SPCE that underwent deconvolution*. (A and B) AP10, (C and D) AP25 and (E, F and G) SN30.
** The sample SN30 presents different agglomerations in each voltammogram. Analysis of the behavior of this sample and the others are detailed in the conclusion section.*

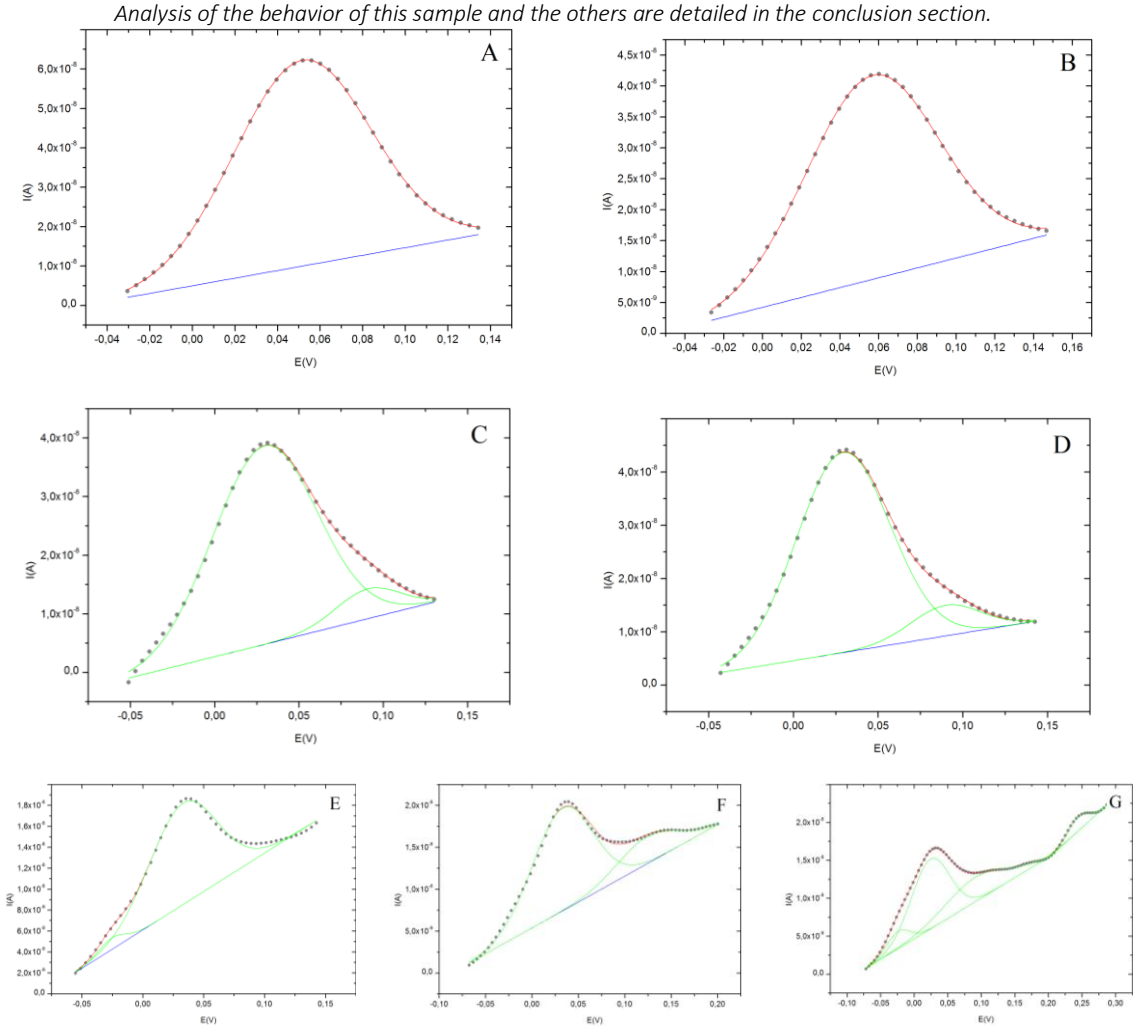

In the **table 5** are collected the results of the samples subjected to deconvolution and the diameters. The inaccuracy of the results is presented by the standard deviation (SD).

Table 5. The table summarizes the average diameter and standard deviation of the sample peaks on modified SPCE after deconvolution. Each value is the average of three different mean values generated after interpolation in the two respective calibration curves. SN30 values are mean values obtained from interpolation in the two calibration curves. The differences between them cannot allow obtain averaged values.[1] The diameters extracted from reference [27] are also shown[2].

Samples	Peaks	Diam. (nm) ± SD	Diam. (nm) ± SD[2]
AP10	1st peak	28 ± 1	52 ± 1
AP25	1st peak	16 ± 0	26 ± 1
	2nd peak	60 ± 1	
SN30[1]	1st voltam	6	28 ± 2
		18	
	2nd voltam	18	
		126	
	3rd voltam	6	
		15	
		60	
		1850	

5.6. CONCLUSIONS

As can be seen, the voltammograms used for deconvolution are different from those observed in the article. The voltammograms used to obtain the diameter of the samples correspond to voltammograms that did not show any evidence of agglomeration or aggregation, that is sharper peaks with no shoulders. The article peaks are narrower because they have no agglomerates. By contrast, the voltammograms of this work are wider and in some of them the presence of agglomerates are clearly observed. Differences in comparing the diameters can be explained on this basis.

The different peaks observed in deconvolution are the result from the formation of agglomerates (weak physical interactions[29]) among AgNPs. The drying process or rate of nitrogen flow, surface covered on the working electrode by the nanoparticles, exposure of them to the light[30], etc. are factors which affecting the stability of AgNPs and for this reason we can see different sizes of agglomerates. Another factor to consider is the ligands used to cover the nanoparticles and keep them stable. In standard solutions used in this work, the AgNPs are citrate capped.[27] However, in the case of the samples we do not know the ligands used to stabilize the nanoparticles because this

information is not provided by the manufacturer. A very important factor that can help us to explain the differences between these two approaches is the material of the electrodes. The shape and the position of the voltammograms on the potential axis are determined by the interactions between the nanoparticles and electrodes.[28]

We also have to take into account, when comparing values of this work with article values, is that the number of data used for averaging are different. This factor may influence the observed differences in the comparison of values.

5.6.1. Samples of AgNPs on Glassy Carbon electrode (GC)

The peaks found in each voltammogram for each sample shows peak potential very similar values. This behavior is the same for all three samples. Standard deviation values are lower for the samples AP10 and SN30. The deviation observed in AP25 sample is due to the factors discussed at the beginning of the conclusions section. It has to be bared in mind that the diameter distribution observed using TEM was broad[27] for all samples, meaning that there is a broad dispersion of particles of different size in all cases.

- AP10: Larger particles agglomerate more easily than small; therefore, the peaks of smaller populations can be distinguished better. This is what happens in this sample and you can see two populations of different sizes.
- AP25: The size obtained is twice the size given in the article and therefore we can think that is agglomeration. However, the inaccuracy is four times higher than in the article. So it is hard to tell if the differences are due to agglomeration.
- SN30: The values obtained are lower than those given in the article. These results can be explained by deconvolution. That is, deconvolution does not fit well the profile peak. It seems there are three peaks, but are difficult to adjust to the peak. The third peak would appear at the end of the peak which is not well adjusted.

5.6.2. Samples of AgNPs on a modified SPCE.

This approach also shows repeatability in the peaks found after deconvolution for two samples, AP10 and AP25. However, the peaks found in SN30 do not exhibit full repeatability. That is, repeatability is biased by the different factors that affect agglomeration that are difficult to control, as a result it can be seen in the **table 5**, two peaks of 18nm (1st and 2nd voltam) Ag nanoparticles and two peaks of 6nm (1st and 3rd voltam) Ag nanoparticles for SN30. It has to be bared in mind that the diameter

distribution observed using TEM was broad[27] for all samples, meaning that there is a broad dispersion of particles of different size in all cases.

- AP10: As in the case of GC, the values obtained are lower than those given in the article. No populations of different sizes are appreciated, it may mean that the sample has been oxidized during this time.
- AP25: The values obtained are higher and lower than those given in the article. This can be explained by the agglomeration of larger particles and allow us to observe the populations of smaller size.
- SN30: In this particular case, each voltammogram gives populations of different sizes. A possible explanation may be that composition itself of the sample is which facilitates the agglomeration. We can not forget that the substrate used is different and can be a possible cause of agglomeration.

Preview information: nanoceria standards.

As it was already mentioned, the chemistry of silver is very advanced, and therefore we have a good control on the AgNPs synthesis process, stabilizers, dispersion medium, etc. Consequently, AgNPs standards of different sizes and shapes are commercially available.[31-33]

However, the chemistry of cerium and its oxides is not well known yet. Besides, we cannot find nanoceria standards of different sizes in the market. The absence of standards makes difficult the use of the method employed for AgNPs. That is, we cannot obtain a calibration plot that allows us to interpolate a certain sample. In view of this difficulty, we are forced to seek alternatives for the characterization of nanoceria. One alternative that can be useful in this task is the *Particle Collision* (PC).

6. CHARACTERIZATION OF NANOPARTICLES BY PARTICLE COLLISION (PC)

6.1. INTRODUCTION

Initial studies about individual electrochemical signals corresponding to small particles were developed by Heyrovský et. al. in 1995.[34-37] Later, Bard and his group are the first to study the particle collision. They studied the impact of different nanoparticles, mainly Pt nanoparticles, with catalysis.[38-41] Subsequently, another studies on the electrochemical signals generated by the impacts of different nanoparticles on the electrodes are developed by G. Compton et. al. between 2011 and 2012.[42-46] Even particles of clays, such as montmorillonite, have been characterized with this technique.[47]

PC is based on measuring the Faradaic current associated to the electrode reaction that takes place when a nanoparticle (NP) hits the surface of a microelectrode (ME). Each collision is observed as a transient signal with an approximate duration of milliseconds, if the nanoparticle does not stick to the electrode, that is the case a step is observed whose height depends on the size of the nanoparticle. This method can be divided in three different approaches (**Figure 8**) according to the electrochemical reaction produced to obtain the signal:

- Direct: The signal is obtained from the direct reaction between the nanoparticle(NP) and microelectrode(ME).[43](**Fig.8A**)

- Electrocatalysis: The signal is obtained more easily by the presence of electrocatalytic active species whose reaction is catalyzed by the NP. These species do not react, or its rate is very low, directly on the ME[39] (**Fig.8B**) This approach is mandatory when the NP is not electroactive or in the case of the destruction of the nanoparticle should be avoided. It is also the way to increase the sensitivity of the procedure because the signal depends on the concentration of the reactive whose electrode reaction is catalized by the NP and the number or electrons exchanged by this reactive. Another way to accomplish these goals is depicted in the next point.
- Tag-redox: Nanoparticles are covered or "tagged" with redox species. The signal is obtained from the reaction between tagged-NP and ME (**Fig.8C**).This is a non-destructive method.[48] This procedure is used when the nanoparticle is not electroactive or just to avoid interferences.

Figure 8. Three different approaches of PC: (A) Direct, (B) Electrocatalysis, (C) Tag-redox.

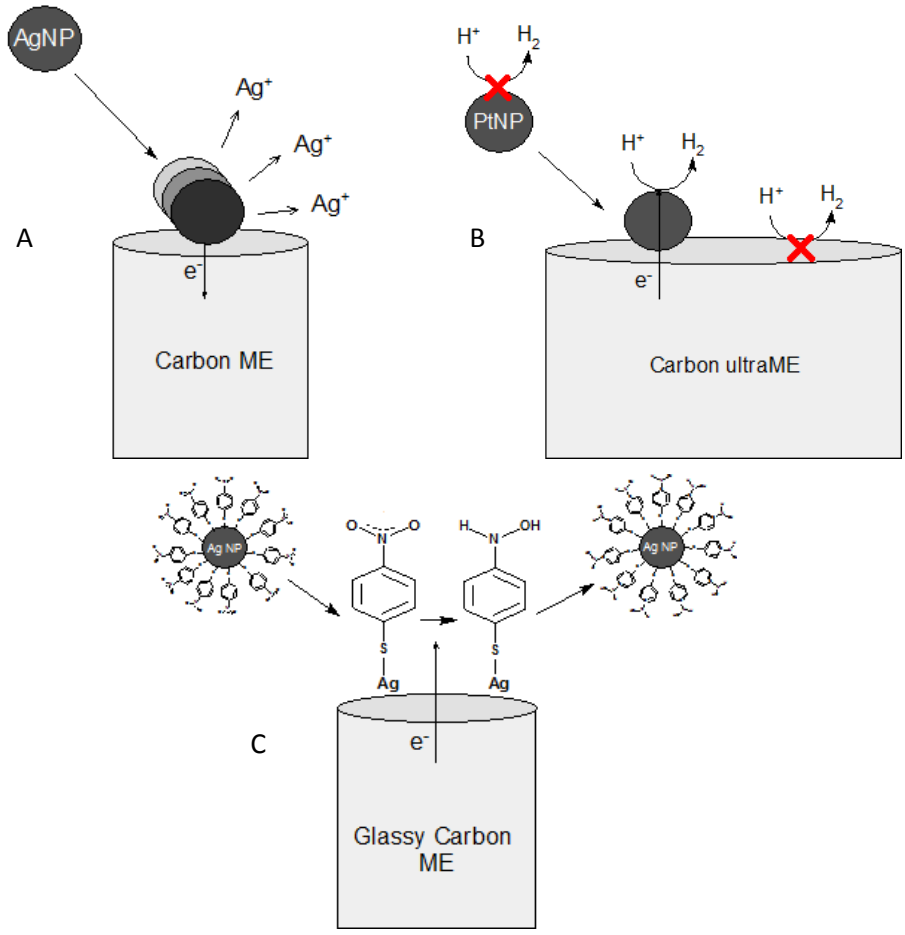

6.2. BACKGROUND NOISE

The "electronic background noise" is produced by electronic interference namely potentiostat itself, computer or power supply. This noise is a relevant problem indeed in this case because the signals generated by the nanoparticles have low intensities (pA) and can be lost in the background noise. Therefore the data must be treated to remove the majority of the electronic noise. The electronic noise is observed as different superimposed waves when the data are drawn in a different software that the used in the potentiostat, so it can be seen in **Figure 9A**. The same data after being treated are shown also in **Figure 9A**.

In the first experiments we could see other noise related with the environment work. In these experiments, the potentiostat was in an area with high traffic of people and vibrations produced by people affect the stability of the background signal. Examples of vibrations can be seen in **Figure 9B**. The solution to this noise was to move the work area to a place with less movement of people.

If the noises are wiped, it is possible to obtain very low and good backgrounds. An example is observed in **Figure 9C** where you can see that the original data did not differ greatly from the treated data as in the case of **Figure 9A**. The data processing is also important because it helps to see hidden peaks under the noise.

Figure 9. (A) Electronic noise, (B) Instability of background by vibrations, (C) Low background signal (original data are shown as black dots and treated data are represented as blue dots).

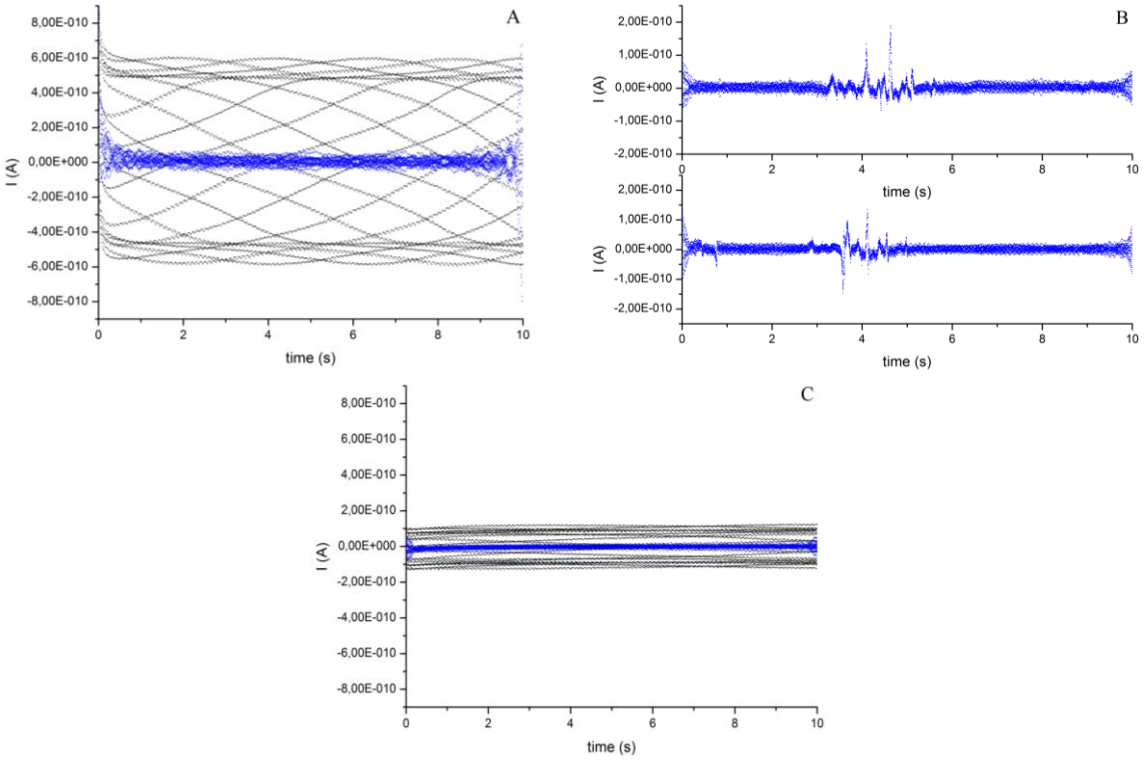

6.3. MATERIALS

Chronoamperometry measurements were carried out with Eco Chemie Autolab PGSTAT-10 with low intensities module and controlled by computer.

Two different WE were used: Glassy Carbon microelectrode (GC-ME) with 11 ± 2µm of diameter and Platinum microelectrode (Pt-ME) with 10µm of diameter. The reference electrode was Ag/AgCl/3M NaCl and auxiliary electrode was a Pt wire (image of these electrodes can be found in annex **A3**). Standard of AgNPs 100nm, ($2{,}73.10^{18}$NP L^{-1} - 20ppm) were purchased from Sigma-Aldrich. Source Naturals 30ppm (SN30, $3{,}03.10^{14}$NP L^{-1}) sample was also used in this section. CeO_2 5% wt aqueous nanoparticle suspension (4nm diameter, $2{,}03.10^{20}$NP L^{-1}) and CeO_2 20% wt in 2,5% acetic acid nanoparticle suspension (10-20nm diameter, $7{,}61.10^{18}$NP L^{-1}) were purchased from PlasmaChem.

The different chemical reagents used are: Anhydrous sodium dihydrogen citrate, NaCl, $NaClO_4$, $NaBH_4$ and L-ascorbic acid. The liquids reagents were: H_2O_2 30% and HCl 35% from Scharlau Chemie. All solutions and dilutions of NPs were prepared with ultrapure water (Mili-Q Advantage)

6.4. PROCEDURE FOR SILVER NANOPARTICLES (AgNPs)

The study was conducted using two of the three approaches mentioned on introduction section: Direct and Electrocatalysis. Platinum microelectrode was used as working electrode in both approaches

6.4.1. Direct

Different procedures were followed for the direct analysis. The results obtained in this approach were not promising in any procedure. Electrolyte or characteristics can be found in the annex **A4**. The parameters used are collected in **Table 6**.

Table 6. Measurement parameters used in Direct PC

E (V)	Measurement duration (s)	Measuring time (s)
0,5	10	0,001
0,5	5	0,0005

General procedure: 10mL of electrolyte solution are deposited in an electrolytic cell. Then, a nitrogen flow is bubbled through the solution for 15-20 minutes to displace oxygen and prevent oxidation of the NPs. At this point, measurements

of blank were performed on the electrolyte alone. The AgNPs 100nm solution, previously sonicated for 1 minute, is injected into the cell and the circuit is completed with working, reference and auxiliary electrodes. The three electrodes are clamped using parafilm to hold them in position and prevent fluctuations in the measurements. Once the circuit is closed, the nitrogen flow is extracted from the solution but not from the cell, thus maintaining a positive pressure inside and prevents the entry of oxygen. Measurement parameters are set and start measuring. The total measurement time is between 3-4 hours but can be extended to higher values. The higher total measurement time, the probability to observe collisions is higher.

6.4.2. Electrocatalysis

In this case, the peaks generated are the results of the electrocatalytic reduction of H_2O_2 on the surface of AgNPs.

As in the previous case, several tests were made and best results were obtained compared with direct detection. The experimental parameters or features are listed in annex **A5**. The parameters used are collected in **Table 7**.

Table 7. Measurement parameters used in Electrocatalytic PC.

E (V)	Measurement duration (s)	Measuring time (s)
-0,9	10	0,001
-0,9	5	0,0005

The general procedure is the same that in the previous case. The main differences are related with potential and electrolyte solution.

The useful results were found followed the parameters or features in annex **A5i**.

6.5. CALCULATION FOR SILVER NANOPARTICLES (AgNPs)

The data were treated with Origin 8.0. The first thing is to clean the data of eddy currents. In order to clean the data, the data at frequencies of 50Hz and 150Hz were extracted to the original data and the final data were used to obtain the area of peaks.

6.5.1. Direct detection of AgNPs

In case of direct oxidation, the charge transferred for each impact (Q) is related to the number of atoms capable of being oxidized (N) by the equation (I).

$$Q = e.N \qquad \text{(I)}$$

where e is the electronic charge.[43,46] Therefore, we can obtain quantitative information of nanoparticles in this case. Furthermore, the charge can also be expressed in terms of the NP radius by the equation (II).

$$Q = \frac{4n\pi\rho F}{3M}\left(r_i^3 - r_f^3\right) \qquad \text{(II)}$$

where n is the number of electrons transferred per atom (n = 1 for silver), ρ is the bulk metal density (10,49 g ml^{-1}), F the Faraday constant (96485 C mol^{-1}), M is the atomic weight of the metal (107, 8683 g mol^{-1}), r_i the initial NP radius and r_f the final NP radius. In this case, the potential used is positive enough to the NP will be completely oxidized and therefore r_f = 0.[43,46]

6.5.2. Electrocatalytic detection of AgNPs

The variation in the charge (Q) depends on H_2O_2 concentration. Assuming full 2-electron reduction of every H_2O_2 molecule, single spherical nanoparticle and purely diffusion-limiting current for the duration of an impact; we can obtain an equation which relates Q, $[H_2O_2]$ and radius of nanoparticle, r, through the equation (III).[49]

$$\frac{Q}{[H_2O_2]} = 4\pi nFDr.\Delta t \rightarrow r = \frac{Q}{4\pi nFD.\Delta t[H_2O_2]} \qquad \text{(III)}$$

Where $[H_2O_2]$ is the hydrogen peroxide concentration (2,80.10^{-27} mol nm^{-3}), n is the number of electrons (2 in H_2O_2 reduction), F is the Faraday constant (96485,3399 C mol^{-1}), D is a diffusion coefficient (assuming a typical value of 10^{-5} cm^2 s^{-1}, 10^9 nm^2 s) and Δt is the peak duration in seconds. So, using the charge passed per peak you can get the radius of AgNPs in nm.

6.6. <u>RESULTS FOR SILVER NANOPARTICLES (AgNPs)</u>

6.6.1. Direct detection of AgNPs

In direct Particle Collision, we did not get any reliable or valid result and therefore we can not show any numerical result.

6.6.2. Electrocatalytic detection of AgNPs

Electrolytic particle collision shows results but they are not very useful for the sample characterization. We can find the radius of NP by this catalysis method with H_2O_2 using equation (III). In this experience, we obtained two peaks (**Figure 10**) and the radii of these AgNPs are collected below (**Table 8**).

Figure 10. Peaks of AgNPs (100nm) observed by Electrocatalytic PC.

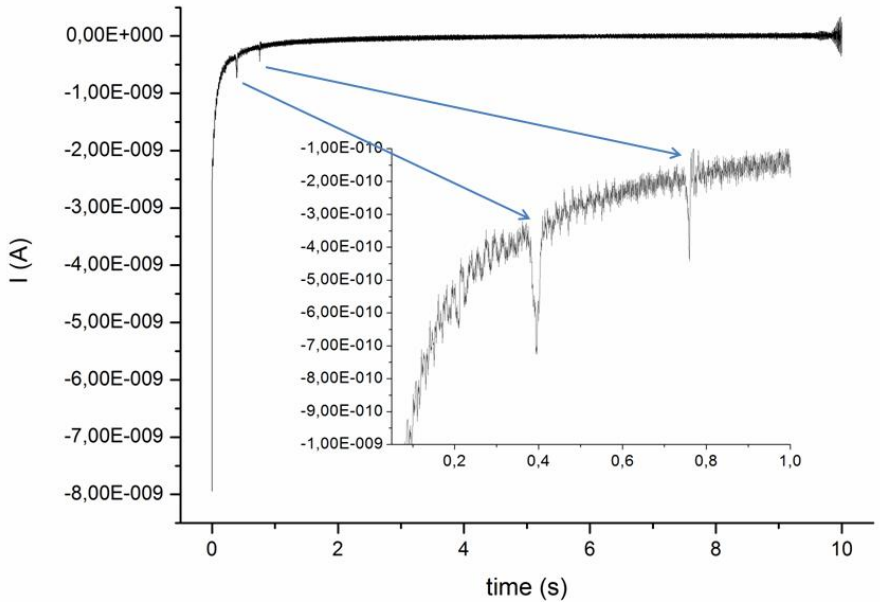

Table 8. AgNPs radius obtained by Electrocatalytic PC.

Peaks	Q (C)	**AgNPs radius (nm)**
1st	$4{,}67.10^{-12}$	**25**
2nd	$1{,}52.10^{-12}$	**17**

6.7. CONCLUSIONS FOR SILVER NANOPARTICLES (AgNPs)

The results generated in the Electrocatalytic approach are not sufficient to get a valid conclusion. The experimental radius is approximately four times lower that the theoretical value. One possible cause of these results is that the impacts correspond to these AgNPs sizes or their size has decreased by oxidation. However, one conclusion that we can get is the catalysis seems to offer better results than direct PC.

It has to be pointed out that the AgNP concentration used in this experiment is high, higher that it is supposed to be in waste waters or in the environment. Beside the time required to obtain a useful number of events is long, up to several hours. It is necessary to increase the number of collisions even with lower concentration of nanoparticles by sizing down the volume of the cell or charging the geometry of the working electrode.

6.8. PROCEDURE FOR CERIA NANOPARTICLES (CeO_2NPs)

The study was performed using two approaches. One approach is Direct particle collision and the other is catalytic reduction when the collision of a nanoparticle takes place. Glassy carbon and Platinum microelectrode were used as working electrode.

6.8.1. Direct particle collision

Several nanoparticles have been detected by Direct PC, however we have not found any reference on the detection of nanoceria by PC. For this reason, this approach was tested in nanoceria in the first place. The characteristics or parameters used in the procedures can be found in the annex **A6**. The general procedure is the same as for the study of AgNPs by PC. It can be described as: 10mL of electrolyte solution are deposited in an electrolytic cell. Then, a nitrogen flow is bubbled through the solution for 15-20 minutes to displace oxygen. The presence of oxygen can influence the reactivity of the nanoceria because it strongly depends on the environment. Then, measurements of blank were performed on the electrolyte alone to control the noise level and be sure that no electromagnetic interferences are present. A low, pA, and stable base line is necessary prior the nanoparticles experiment. Nanoceria suspension, previously sonicated for 1 minute, is injected into the cell and the circuit is completed with working, reference and auxiliary electrodes. The three electrodes are clamped using parafilm to hold them in position and prevent fluctuations in the measurements. Once the circuit is closed, the nitrogen flow is extracted from the solution but not from the cell, maintaining a positive pressure inside and preventing the reequilibrium with oxygen. Measurement parameters are set and the measurement is started. The total measurement time can be 2-4 hours but it can be longer. The higher the total measurement time, the higher probability of observing more collisions.

Valid results were obtained following the general procedure with parameters collected in **A6ii**. Forty-three peaks were extracted in 52 measurements and some of these peaks are shown in annex **A8**. The parameters of this procedure are collected in **Table 9**.

Table 9. Parameters and features used in the procedure which gave successful result by Direct PC.

E (V)	-0,5
Measurement duration (s)	10
Measuring time (s)	0,001
Electrolyte	10mL 1M HCl
Working electrode	Glassy carbon ME
Nanoceria diameter	4nm
[CeO_2NPs]	1000ppm
NP L^{-1}	$3{,}9.10^{18}$

6.8.2. Particle collision with catalytic reduction.

From the literature we know that nanoceria modified through a treatment with hydrogen peroxide can be followed by PC due to the catalytic reduction of the peroxo and superoxo groups O_2^-/O_2^{2-} that are bonded on its surface.[50] Hydrogen peroxide (H_2O_2) is used to modify the surface of nanoceria using their property as free radical scavenging.[11] (**Figure 11**)

Figure 11. Scheme and reaction produced in particle collision with catalytic reduction (surface modification in nanoceria).

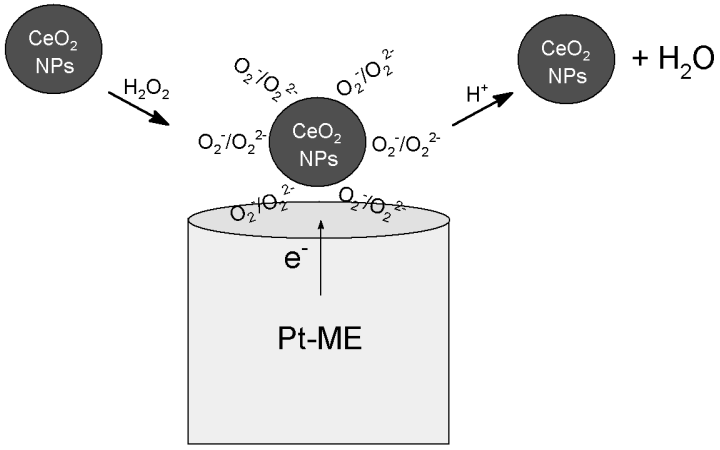

$$CeO_2 + H_2O_2 \rightarrow Ce_2O_3 + O_2 + H_2O$$

$$Ce_2O_3 + O_2^-/O_2^{2-} + 2H^+ \rightarrow 2CeO_2 + H_2O$$

Several tests were made and best results were obtained compared with direct approach. The experimental parameters or features are listed in annex **A7**. This approach also was performed successfully, besides the results were useful to characterize nanoceria since a size distribution was obtained. The general procedure is the same that in the previous case but some differences have to be

mentioned like WE preparation, working potential and electrolyte solution, see **Table 10**. A certain volume of hydrogen peroxide is added and the surface of WE is chemically activated. Fifteen minutes before measuring, WE (Pt-ME) was immersed in solution of 10mM $NaBH_4$ in order to reduce the platinum oxides always present on the electrode surface (WE activation). After this time, the microelectrode was washed with mili-Q water and placed in the electrochemical cell with the other two electrodes. The added H_2O_2 produced changes in the color of the solution. The change from colorless to yellow (see **Figure 12**) is due to the oxidation of Ce(III) to Ce(IV) state on nanoceria surface.[15]

Figure 12. Image of nanoceria solution after that H_2O_2 is added.

Successful results were obtained following the general procedure with parameters collected in **A7iii**. Two hundred eighty-five peaks were extracted in 100 measurements, some of these peaks are shown in annex **A9**. The parameters of this procedure are collected in **Table 10**.

Table 10. Parameters and features used in the procedure which gave successful result by particle collision with catalytic reduction.

E (V)	-0,2
Measurement duration (s)	10
Measuring time (s)	0,001
Electrolyte	10mL – 1M HCl / 10mM H_2O_2
Working electrode	Platinum ME
Activation WE	15 min in 10mM $NaBH_4$
Nanoceria diameter	4nm
[CeO_2NPs]	990ppm
NP L^{-1}	$3{,}86.10^{18}$

Due to the good results given by this method, nanoceria standard of 10-20nm also was tested but successful results were not obtained. We think that the problem is the dispersion medium (2,5% acetic acid) and different procedures and electrolytes were tested with this standard (annex **A7**). The procedure does not show repeatability and others parameters and features of the general procedure were tested: decreasing the volume of electrolyte (decrease the path traveled by the NP), changing the superficial reaction (searching for another more repetitive reaction), change the reducing agent, centrifugating the nanoparticles after exposure to hydrogen peroxide to remove the excess of peroxides that can be harmful to nanoceria[50], after precipitation with NaCl. All of them are collect in the annex with the comments and results in each case.

Other collisions of 4nm nanoceria are observed with the procedure **A7xi** using directly $NaBH_4$ to activate the surface of nanoceria by generating more Ce(III). Only 11 peaks were extracted, which are not useful for size distribution. Some of these peaks are shown in annex **A12**.

Another experiment which also gave some results for 10-20nm nanoceria is summarized in procedure **A7xii** and **A7xiii**. Good results were obtained in two repetitions, but they are not enough data to give a size distribution. Some peaks are shown in annex **A13**.

At this point, one important issue for the proper development of PC in nanoceria is that we do not really know which is the Ce(III)/Ce(IV) ratio in nanoceria. This is an important factor to consider since its chemical activity depends on this ratio.[13-15]

From the experiments performed with borohydride we can conclude that the ratio Ce(III)/Ce(IV) is critical and that increasing the amount of Ce(III) the PC experiments shows more collision events. But as borohydride is a strong reducing agent it can reduce ceria and also other unwanted species, that resulted in an oxidation peak of unknown nature during a PC experiment that can be seen in annex **A13**. Consequently, another reduction agent, milder than borohydride is necessary. Ascorbic acid is known to be oxidized by nanoceria[51] and selected to perform our experiment. UV-visible was used in order to get a closer look at the nanoparticle Ce(III)/Ce(IV) ratio using ascorbic acid.

6.8.3. Study UV-visible of 10-20nm nanoceria

The objective of this study is to determine if the ascorbic acid (AA) can act as an alternative to the borohydride studying its influence on the peaks of Ce(IV) and Ce(III) observed on the spectra. Reference [15] cite: "*The first peak is in the 230-260nm range and corresponds to cerium(III) absorbance. The second peak absorbance occurs in the 300-400nm range and corresponds to cerium(IV) absorbance*" and this will be useful to get an idea of the relative abundance of Ce(IV) and Ce(III). AA is unstable and must be kept away from light, heat or oxygen. Therefore, it must be handled with care. 1410ppm of 10-20nm nanoceria solution was used, the concentration of AA was 1, 2, 4, 6 and 8mM and 0,1M HCl was used as media. Spectrum was performed from 200 to 1100nm in glass cuvette. A spectrum of HCl was remained as blank. Appropriate volumes of nanoceria, AA and HCl were added for each case and then were measured every 5 minutes until 20 minutes. These intervals were to observe possible changes in the spectra as a function of time. The volumes used are collected in **Table 11**.

Table 11. Volumes of nanoceria, AA and HCl used to perform UV spectra.

Experiments	µL of 24400ppm nanoceria	µL of 21645ppm ascorbic acid (AA)	µL of 0,1M HCl
NPs + 0mM AA	87	---	1413
NPs + 8mM AA	87	100	1313
8mM AA	---	100	1400
NPs + 6mM AA	87	73	1340
6mM AA	---	73	1427
NPs + 4mM AA	87	49	1364
4mM AA	---	49	1451
NPs + 2mM AA	87	24	1389
2mM AA	---	24	1476
NPs + 1mM AA	87	13	1400
1mM AA	---	13	1487

Two peaks are observed on the spectra, one at 295nm corresponding to Ce(III) and another one at 390nm that is related to Ce(IV).[13,15] Both peaks are present from the beginning. The peak at 390nm overlaps with AA peak but the peak at 340nm is not.

6.9. CALCULATION FOR CERIA NANOPARTICLES (CeO_2NPs)

As in the AgNPs, data were treated with Origin 8.0. The first thing is to clean the data of eddy currents. In order to clean the data, the data at frequencies of 50Hz and 150Hz were extracted to the original data and these data were used to obtain the area of peaks.

6.9.1. Nanoceria by Direct Particle Collision

To calculate the radius from the charge passed (Q) we can follow the instructions in **Scheme 1** (assuming that whole NP participating in the reaction, not only the surface).

Scheme 1. How obtain the radius of nanoceria from the charged passed by Direct PC.

$$Charge(C) \xrightarrow{F=96485\frac{C}{mol}=\frac{Charge}{mol}} mol_{CeO_2} \xrightarrow{MW_{CeO_2}\left(\frac{g}{mol}\right)} mass_{CeO_2(g)}$$

$$\xrightarrow{\rho\left(\frac{g}{ml}\right)} Vol_{CeO_2}(ml) \xrightarrow{Vol_{CeO_2}=\frac{4}{3}\pi r^3} r(cm) \xrightarrow{r(cm)*10^{21}\frac{(nm)}{(cm)}} r(cm)$$

where charge is obtained experimentally by the area under peak, molecular weight (MW) of CeO_2 is 172,115 g mol^{-1} and ρ is the density of CeO_2 with 7,215 g mL^{-1}.

6.9.2. Nanoceria by catalytic reduction particle collision.

Assuming full 2-electron reduction of each peroxo group ($O_2^{2-} + 4H^+ + 2e^- \rightarrow 2H_2O$), single spherical nanoparticle and purely diffusion-limiting current for the duration of an impact; we can obtain a equation which relates Q, $[H_2O_2]$ and radius of nanoparticle through the previous equation (III).[49]

$$\frac{Q}{[H_2O_2]} = 4\pi nFDr.\Delta t \rightarrow r = \frac{Q}{4\pi nFD.\Delta t[H_2O_2]} \qquad \text{(III)}$$

Where $[H_2O_2]$ is the hydrogen peroxide concentration (1.10^{-26} mol nm^{-3}), n is the number of electrons (2 in this case), F is the Faraday constant (96485,3399 C mol^{-1}), D is a diffusion coefficient (assuming a typical value of 10^{-5} cm^2 s^{-1}, 10^9 nm^2 s) and Δt is the peak duration in seconds.

Once obtained the radii of nanoceria, the next step is to make the analysis of frequencies and their representation or size distribution. A minimum amount of 100 data are required to do size distribution. If there are agglomerations or aggregations more data are needed.

6.10. *RESULTS FOR CERIA NANOPARTICLES (CeO_2NPs)*

6.10.1. Nanoceria by Direct Particle Collision

Forty-three peaks were extracted in 52 measurements. The radii of each peak or collision are obtained following the instructions of the **Scheme 1**. The radii and frequency analysis for size distribution are collected in **Table 12**. Likewise, **Figure 13** shows the graph of the size distribution.

Table 12. Radii and frequency analysis of nanoceria by Direct PC.

Nº of peaks	r (nm)	Nº of peaks	r (nm)	Nº of peaks	r (nm)
1	30	16	46	31	29
2	47	17	26	32	35
3	23	18	20	33	29
4	33	19	54	34	35
5	42	20	27	35	29
6	39	21	24	36	33
7	21	22	36	37	29
8	31	23	36	38	35
9	17	24	51	39	66
10	26	25	46	40	65
11	46	26	38	41	44
12	67	27	28	42	27
13	32	28	52	43	49
14	55	29	53		
15	37	30	27		

Range (nm)	Freq.
10	0
20	1
30	14
40	13
50	7
60	5
70	3
80	0

Figure 13. Size distribution of 4nm nanoceria obtained by Direct PC.

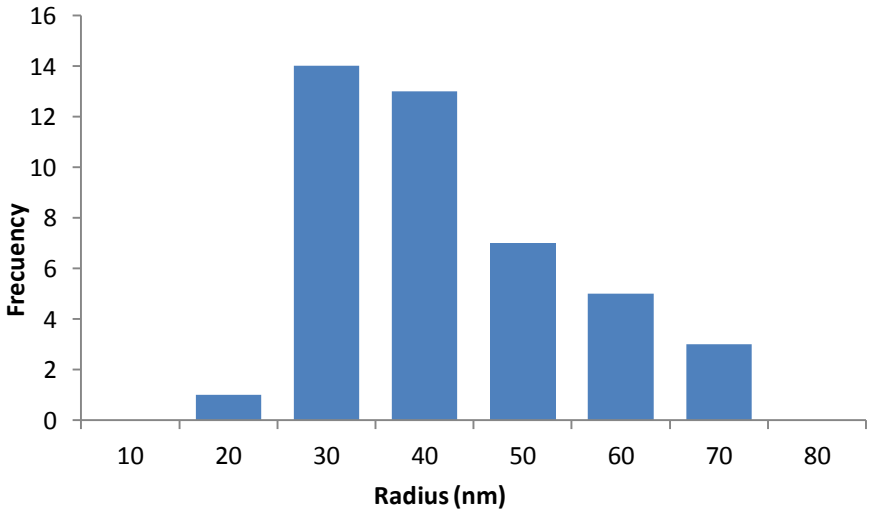

6.10.2. Nanoceria by catalytic reduction particle collision.

Two hundred eighty-five peaks were extracted in 100 measurements. The radii of nanoceria were obtained through the equation (III). The radii of nanoceria not shown here but are listed in the annex **A10**. The frequency analysis is collected in **Table 13** and **Figure 14** shows the graph of the size distribution.

Table 13. Analysis of frequencies in 4nm nanoceria by Electrocatalytic PC.

Range (nm)	Frequency
2	23
4	139
6	76
8	18
10	15
12	5
14	1
18	1
20	3
22	1
40	1
44	1
66	1

Figure 14. Size distribution of 4nm nanoceria in Electrocatalytic PC.

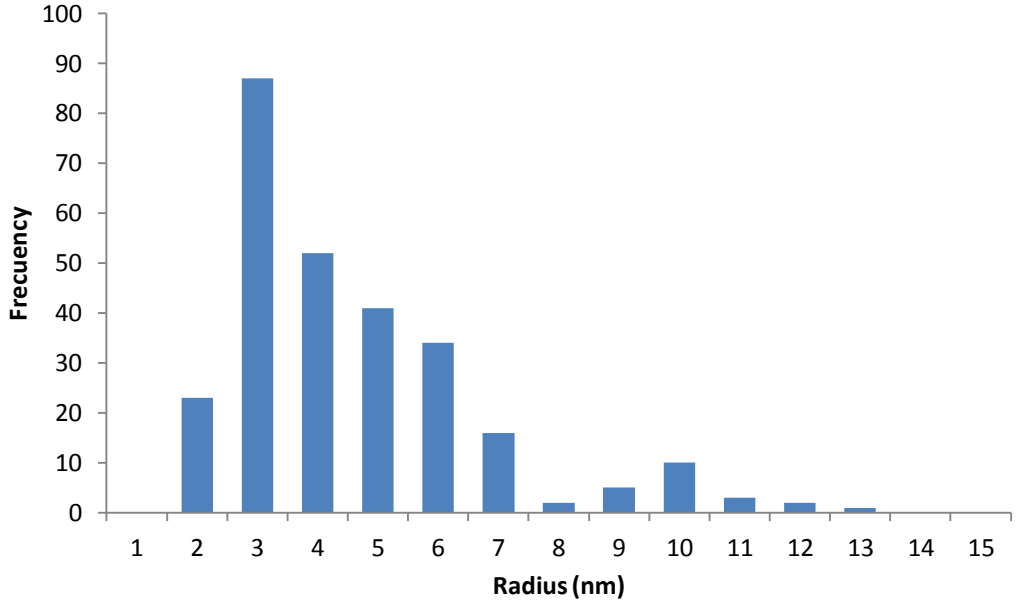

6.10.3. Study UV-visible of 10-20nm nanoceria

The spectra measured of each AA concentration to intervals of 5 minutes are listed in annex **A11**. **Figure 15** shows an overall graph of the initial spectra at each concentration of AA.

Figure 15. UV-visible spectra of 10-20nm nanoceria with different concentrations of AA.

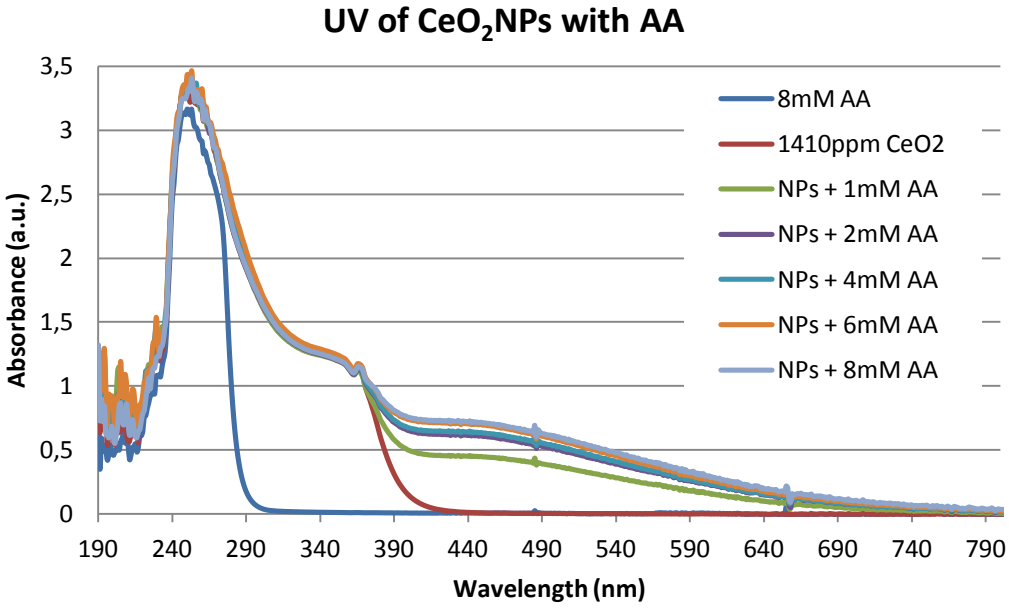

6.11. CONCLUSIONS FOR CERIA NANOPARTICLES (CeO_2NPs)

6.11.1. Nanoceria by Direct Particle Collision

The experimental value is around 30-40nm, which is far from the theoretical value of 4nm. There are three factors that have to be considered: First, the size distribution is made with 43 data and the minimum amount required are 100 data. Second, we have assumed that whole nanoparticle is responsible for the charge exchange with the electrode, that should not be completely true. Beside not all cerium is as Ce(IV), so the theoretical value of total charge exchanged per particle might be overvalorated. Third, the optimal ratio nanoparticle diameter/working electrode diameter should be 1/1000. It makes extremely difficult to detect a 4nm particle impact on a 10µm electrode. Consequently, it is easier to detect the biggest particles present in the suspension, that is to say 30 to 40nm as it happened in our experiment unless an increase of sensibility is attained. That is why we turned to a catalytic reaction coupled with particle collision.

6.11.2. Nanoceria by catalytic reduction particle collision.

A good nanoceria size distribution was obtained with this approach due to the large amount of data. The PC results give a distribution that is between 2 and 7nm with the highest value of 3nm. If we compare the result (3-4nm) with the value provided by the manufacturer (4nm), we can see that the difference is very small. Another comparison can be made with data from TEM images. Images from TEM and distribution are collected in annex **A14**. The size distribution obtained from TEM gives a size around 1 and 5nm with the highest value at 3nm. The result of TEM (2-3nm) can also validate the result of PC (3-4nm). A second size distribution around 10nm can be seen in **figure 14**. This second distribution may be the result of an agglomerate. Distribution obtained by TEM does not give the second distribution of 10nm because the preparation of the TEM sample is made in their medium. In our case, nanoceria are dispersed in 1M HCl (pH 0) which modifies the surface and could be possible that NPs agglomerates.

The supporting electrolyte in which are suspended the nanoparticles as well as the capping agent influence decisively the effectiveness of the chronoamperometric procedure. For this reason, the results obtained for 10-20nm nanoceria were unsuccessful. Direct particle collision events can be detected if the number of Ce(III) atoms is increased using strong reducing agents. The measuring time affects the noise. The longer the measuring time the better. But this parameter should be short enough to allow the detection of a single particle collision event to be detected. A compromise situation should be accepted

6.11.3. Study UV-visible of 10-20nm nanoceria

Nanoceria shows two characteristic regions: one is between 240-290nm and the other regions is between 290-390nm. These peaks are related with Ce(III) and Ce(IV), respectively.[15] However, nanoceria reacted with AA shows another peak around 400-500nm. This peak can be related with agglomeration. AA reacts with the nanoparticles and the products of the reaction can be adsorbed on the surface causing agglomeration.

7. GENERAL CONCLUSIONS

7.1. VOLTAMMETRY IMMOBILIZED PARTICLES (VIP)

VIP has proven to be useful and reliable technique when the reaction processes on the electrode surface are known. The technique has great progress and a lot of articles have been published using this technique. The procedure is simple and the relationship between the analytical signal and the size of the nanoparticle is well documented and studies by several groups. It also allows the study of aggregation/agglomeration processes on the electrode surface, that depends on the nature of this surface. Using a deconvolution algorithm it is possible to know the diameter of the agglomerates. But it requires many standards of nanoparticles with well characterized diameter.

7.2. PARTICLE COLLISION (PC)

Particle collision has proven to be a useful tool to characterize the size of the nanoparticles in a concentrated suspension of nanoceria. The technique provides a view from inside the solution, detecting the formation of agglomerates/aggregates depending on the media conditions (redox potential, ionic strength, pH). PC itself is not a sensitive technique, it requires a high concentration of nanoparticles which limits its use to characterize the behavior of nanoparticles in controlled media for theoretical studies rather than to study them in real samples where concentrations are far below this limit. The sensitivity of the technique can be improved by coupling PC with catalytic reduction.

8. ANNEXES

A0 *Paper of previous work based in AgNPs on GC and SPCE. Reference [27].*

This work is based on characterization of AgNPs on real samples by linear voltammetry.

Analytical Methods

PAPER

View Article Online
View Journal | View Issue

Silver nanoparticle detection and characterization in silver colloidal products using screen printed electrodes

Cite this: *Anal. Methods*, 2014, **6**, 3072

G. Cepriá,* W. R. Córdova, Javier Jiménez-Lamana, Francisco Laborda and J. R. Castillo

Received 9th January 2014
Accepted 22nd February 2014

DOI: 10.1039/c4ay00080c

www.rsc.org/methods

Silver nanoparticles (AgNPs) were detected and characterized in several silver colloidal products available on the market. The relationship of the diameter of the nanoparticle with the corresponding peak potential was used to determine the dimensions of AgNPs in real samples. Quantitative analysis was carried out by voltammetry of immobilized particles on screen printed and glassy carbon electrodes. Screen printed electrodes were used prior to modification of the reference electrode to attain stable readings of peak potential. The repeatability of the modification as well as the quantitative results was checked and found satisfactory.

Introduction

Silver nanoparticles have been used in all aspects of our day to day life but little care has been paid until now to what happens to them once they have accomplished their purpose, becoming waste products. Detection and characterization of nanoparticles in the environment as well as in the daily use products are more necessary than ever.

When dealing with nanoparticles it is necessary to answer three relevant questions, what is their nature, how many, and which size because their properties and their role as environmental hazards depend on them.[1] Especially, the size has been proven to be the main factor since their biotoxicity depends critically on it.[2]

Many different attempts have been made involving different techniques to characterize nanoparticles. Among them, the most frequently used techniques are Transmission Electron Microscopy (TEM), Dynamic Light Scattering (DLS), X-Ray Diffraction (XRD) and many others which were described and compared in the previous literature[3] and more recently field flow fractionation (FFF).[4] FFF exhibits remarkable features when it is coupled with ICP Mass Spectrometry (ICP-MS)[5] that allows concentration and size determination at very low levels and down to 10 nm particle diameter. ICP-MS has also proven to be an interesting tool for the detection of single nanoparticles, in particular silver nanoparticles (AgNPs), and to distinguish them from Ag(I). It also goes one step further by offering data about the particle size and the polydispersity of the sample.[6]

Instituto Universitario de Ciencias Ambientales (IUCA), Grupo de Espectroscopía Analítica y Sensores (GEAS), Facultad de Ciencias, Universidad de Zaragoza, Calle Pedro Cerbuna 12, 50009 Zaragoza, Spain. E-mail: gcepria@unizar.es

Anodic particle coulometry (APC) is a methodology developed in 2011 by Compton and co-workers based on the measurement of the Faradaic charge transfer when a nanoparticle hits the electrode surface set on an adequate potential at which the metallic nanoparticle is destructively and quantitatively oxidized.[7] It is an alternative tool since it provides information about the size and size distribution of nanoparticles and their concentration. It also provides insights into the behaviour of the nanoparticles, their aggregation and evolution in the solution.[8–10]

Voltammetry of immobilized particles (VIP) developed by Scholz in the 90s[11] and adapted for the study of nanoparticle oxidation on an electrode has been used to study the relationship between size and peak potential.[12–14] Few microliters of a sample containing nanoparticles are cast on a graphite electrode surface and allowed to dry. Then, the electrode is transferred to a suitable supporting electrolyte and a voltammogram is obtained. The oxidation potential of an isolated metal nanoparticle is lower than the redox standard potential of the bulk metal depending on the radius and the surface energy of the nanoparticle.[15] Surface interactions between the electrode material and the nanoparticle affect the oxidation potential shifting its value according to the surface Gibbs free energy. If this value is positive, the metal does not interact with the electrode material and the oxidation potential shifts with decreasing radius towards lower values than the bulk oxidation potential of the metal nanoparticle.[16] Theoretical studies have been developed to explain the experimental data through mathematical models that consider these factors, whose purpose is to describe the electrochemical and surface energy properties of the nanoparticles.[13,14]

Surface coverage is another factor that should be accounted for to explain the oxidation voltammograms of metal

nanoparticles. The diffusion of the oxidation products away from the nanoparticle should be considered since it affects the peak potential at the reversible limit. If particles are too close, then the diffusion layers of the neighbour nanoparticles overlap and this affects the position of the corresponding oxidation peak which shifts towards more positive values. In the irreversible limit, the peak potential is independent of the surface coverage.[12,17]

A glassy carbon electrode has been used in most of the experiments but the working electrode of a screen printed set has been successfully used to study the processes taking place at the electrode surface. Here we propose the use of screen printed electrodes instead of the traditional bulk experiment in a three electrode cell. To achieve this goal, a more stable and reproducible reference electrode is needed. Over the years many different methods to produce stable all solid reference electrodes have been proposed[18–20] and nowadays they can be bought from some purveyors. The simplest procedure consists of developing a layer of AgCl on the Ag pattern of the pseudoreference electrode and then covering it with a polymer layer that contains chloride and a protective external layer to prevent chloride from diffusing away.[21] A simple but efficient proposal was offered by Nolan *et al.*[22] They covered Ag/AgCl wire with Nafion containing chloride and obtained an all solid state reference electrode stable enough to be used for the voltammetric determination of Hg in natural waters at a ppb level.

All things considered, electroanalytical techniques are a unique tool for the study, detection and characterization of nanoparticles in all kinds of samples. Voltammetry of immobilized particles (VIP) and APC have been successfully applied to the detection, identification and sizing of silver nanoparticles in a colloidal silver spray available in the market.[23] The detection of AgNPs in environmental samples has been successfully performed using a chemically modified glassy carbon electrode with cysteine that is able to bind AgNPs and concentrate them on its surface,[24] which opens a door to the design of sensors for field analysis.

The authors present here a methodology to detect and identify silver nanoparticles in real samples providing information about their concentration and size using VIP with GC and SPEs for the first time. The use of disposable mass produced devices simplifies the procedures and enables their use for field analysis, since the SPE instrumental design is small enough to make it portable and the adequate selection of the voltammetric technique allows the user to attain very low limits of detection to cope with environmental analysis requirements and convenient selectivity.

Experimental

Reagents and instrumentation

All reagents were of analytical grade. Suspensions of 20 ± 5, 40 ± 5, 60 ± 5 and 80 ± 7 nm silver nanoparticles were purchased from BB International (Cardiff, UK); the suspension of 10 nm was provided by PlasmaChem GmbH and the 100 nm suspension by Sigma. Diluted suspensions of silver nanoparticles were prepared from commercially available suspensions after 1 minute sonication. All of them were prepared with ultrapure water (Milli Q Advantage) and stored in the dark at 5 °C. They were sonicated for just 1 min before their use; care should be taken not to heat the nanoparticles to avoid oxidation. Standards were periodically checked using cathodic voltammetry for Ag(I) detection as described in "AgNP and Ag(I) detection". They were discarded when Ag(I) was detected.

Three different samples purchased from specialized health care shops were studied. These samples were kept in a dark place at room temperature. Dilution with ultrapure water was performed when necessary after one minute sonication. Diluted samples were kept in the dark at 5 °C and sonicated for 1 min prior to use. Sonication periods longer than 1 min are not recommended due to the heating of the sample. The power of the ultrasonic bath used for all these experiments was 50 W.

To determine the diameter of the samples, Transmission Electron Microscopy (TEM) was performed with a JEOL-2000 FXII. 10 μL of the sample were deposited on a 400 mesh grid and allowed to dry.

The silver concentration of the samples was determined by ICP mass spectrometry (ICP-MS) using a Perkin-Elmer Sciex model ELAN DRC-e.

Voltammetric measurements were carried out with a computer controlled AutoLab PGSTAT-12 potentiostat (Utrecht, The Netherlands) connected to three electrode screen-printed carbon electrodes (SPCEs) or to a 10 mL voltammetric cell with an Ag/AgCl/3 M NaCl reference electrode from BAS, Pt auxiliary electrode and glassy carbon (GC) electrode, 3 mm diameter. The diameter of the working electrode in SPCEs was 4 mm. Working and auxiliary electrodes were printed from a carbon-based ink (Gwent, C2091208D1) and the pseudoreference electrode with a silver-based ink.

Procedure

The silver contents of commercial suspensions were determined by acid digestion followed by ICP-MS determination. Aliquots of each suspension (1 g) were placed into PTFE beakers, 1 mL of concentrated HNO_3 was added and the mixture was heated in a sand bath to almost dryness. The digested sample was diluted up to 200 mL with 1% (v/v) HNO_3. Analysis was performed in duplicate.

To perform voltammetric studies, 3 μL of a suspension were drop cast on the working electrode. The drop was placed just on the graphite disk. It has to wet just the graphite surface and should not reach the polymeric substrate or electrodes. Then the drop was dried under nitrogen flow avoiding its displacement or a fast drying that should result in loss of material and aggregation.

The electrochemical cell was filled with 10 mL of 0.1 M $KClO_4$ as the supporting electrolyte to obtain the voltammograms with the GC electrode.

Whenever SPEs were used, 70 μL of 0.1 M $KClO_4$ were deposited to fully cover the three electrodes and the voltammogram was recorded. If the SPE was to be reused, it was carefully rinsed with Milli Q water and allowed to dry at room temperature.

Linear sweep voltammetry was used in all instances; scan speed, 20 mV s^{-1}.

All the electrochemical measurements were performed five times and analyses were performed in duplicate.

Results and discussion

Screen printed electrode modification

To relate the peak potential to the diameter of the nanoparticles, stable and reproducible potential measurement is necessary. The reference electrode of our screen printed electrodes (SPEs) is made from a silver ink and it is not stable enough to achieve reliable and reproducible peak potential measurement only dependent on the surface coverage and the particle diameter. A modification of the screen printed electrodes is necessary. This modification should be simple enough so that it needs just a few minutes and if possible, requiring just one or two steps. Two options were tested, deposition of an agar electrolyte layer or a Nafion film on a chemically or electrochemically deposited layer of AgCl.

We found the chemical way to be a simpler solution for the deposition of an AgCl layer, whose thickness was controlled by the exposure time and concentration of the reagent, 1 M $FeCl_3$ in our case.

A 3 μL drop of 1 M $FeCl_3$ was deposited on the pseudoreference electrode for 1 min to develop an AgCl layer and then thoroughly rinsed with Milli Q water to remove the excess reagent and was allowed to dry under a nitrogen atmosphere.[19] On this layer, two different chloride containing layers were tested, agar and Nafion.

A 3 μL drop of KCl saturated agar was deposited on the Ag/AgCl and allowed to dry at room temperature. The resulting device was tested with a 10 nm solution of AgNPs but it was discarded straight away because the agar layer peeled off after the first measurement. A third layer of a polymer should be necessary to keep it in its place. For the sake of simplicity, this option was disregarded and the Nafion layer option[22] was investigated.

A 3 μL drop of 5% Nafion in ethanol saturated with KCl was placed on top of the Ag/AgCl layer and allowed to dry at room temperature. The screen printed device was tested through 12 voltammograms and the polymeric layer was kept in place. To check the repeatability of the modified device, 10 SPEs were modified and tested using 3 μL of 1 mg L^{-1} AgNPs (60 nm). Twelve measurements were performed with each electrode. The peak potential was 0.055 ± 0.006 V.

The comparison between the three types of SPE is shown in Table 1. We concluded that the Nafion modified SPE offered repeatability and stability of the peak potential measurement, so, it was selected for the study of the samples.

Since the geometric area of the screen printed working electrode was similar to that of the glassy carbon electrode, the same considerations were followed for surface coverage.

AgNP and Ag(I) detection

The presence of AgNPs in the samples was determined by anodic voltammetry of a 3 μL drop of the undiluted sample cast on the glassy carbon electrode and allowed to dry under a N_2 atmosphere to avoid oxidation from atmospheric oxygen. Then a voltammogram is obtained from 0.0 V to 0.8 V at 20 mV s^{-1} scan rate in 0.1 M $KClO_4$. All the samples showed a characteristic anodic voltammogram of AgNPs.

Table 1 Stability and reproducibility of peak potential measurements. Each screen was used for 12 measurements but the one sporting the agar modification that stood only for one experiment. 3 μL of 1 mg L^{-1} AgNPs of 10 nm were deposited on the working electrode for each measurement. Results are mean ± standard deviation

Device	Without modification (V)	Nafion modification (V)	Agar modification (V)
Screen 1	0.023 ± 0.009	0.020 ± 0.006	0.074
Screen 2	0.063 ± 0.008	0.021 ± 0.006	—

The same procedure was used to detect the presence of Ag(I) but a cathodic scan was performed instead. Ag(I) standards of decreasing concentrations were prepared to determine the minimum concentration that resulted in a peak. The minimum detectable concentration was 5 μM. The cathodic voltammograms of all the samples did not show any peak and they were coincident with a blank voltammogram.

No influence of Ag(I) on the reference electrode potential was expected when using the modified SPE.

Size characterization

TEM images were used to determine the size and shape of the nanoparticles in the samples. As it can be seen in Fig. 1 the silver nanoparticles exhibit a rounded shape. It can be observed that the nanoparticles of these samples are covered with a non-metallic layer. The diameter of nanoparticles in sample AP10 is between 10 nm and 50 nm, in sample AP25 between 10 nm and 30 nm and in sample SN30 between 20 nm and 30 nm.

For a determined electrode material, the peak potential depends on the size of the nanoparticle and the surface coverage of the electrode if the electrode process is reversible. If the coverage is kept constant and as low as possible in order to get particles diffusionally independent of each other with a radial mass transport from the NP, the peak potential can be used to estimate the diameter of the attached nanoparticles (di). In this case, there is a linear relationship between the peak potential and ln di with a slope of $2RT/nF$, with $n = 1$ in our case.

The dependence of peak potential with radii of the nanoparticles was studied using the glassy carbon electrode, as a reference procedure, and the screen printed electrode. The calculated diameters were compared with those obtained by TEM.

First of all, a suitable concentration of AgNPs in the diluted suspension was selected to obtain peaks whose peak potential depends only on the particle diameter. 3 μL of suspensions of different concentrations of the standards were cast on the electrode surface and allowed to dry under a nitrogen flow. The peak potential was measured and its relationship with the oxidation charge of the particles deposited on its surface was studied. As the particle coverage is decreasing, the particle size

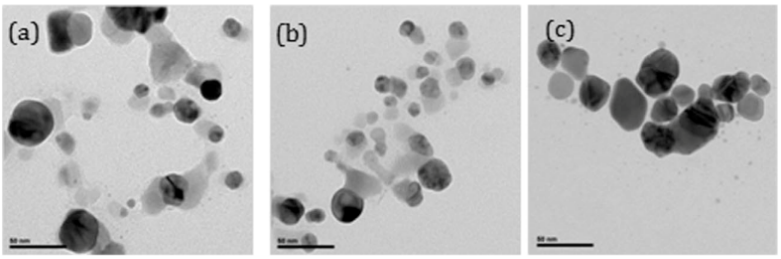

Fig. 1 TEM images obtained from (a) AP10, (b) AP25 and (c) SN30.

becomes the main factor that affects peak potential. When a suitable value is reached the peak potential is governed by the size of the nanoparticles. It was found that whenever the concentration was lower than 2 mg L^{-1} of Ag, the peak potential was independent of surface coverage, see Fig. 2.

To choose the dilutions of the samples, dilutions with MilliQ water were performed until constant potential was attained. It was attained when the natural logarithm of the peak charge, ln Q, was lower than −14. Dilution also helped to diminish the effect of the sample matrix, lowering the baseline and minimizing agglomeration especially when SPEs were used.

The diameter calibration was performed using 0.5 mg L^{-1} dilution of the standards. Five measurements were performed for each standard. The calibration was performed in duplicate.

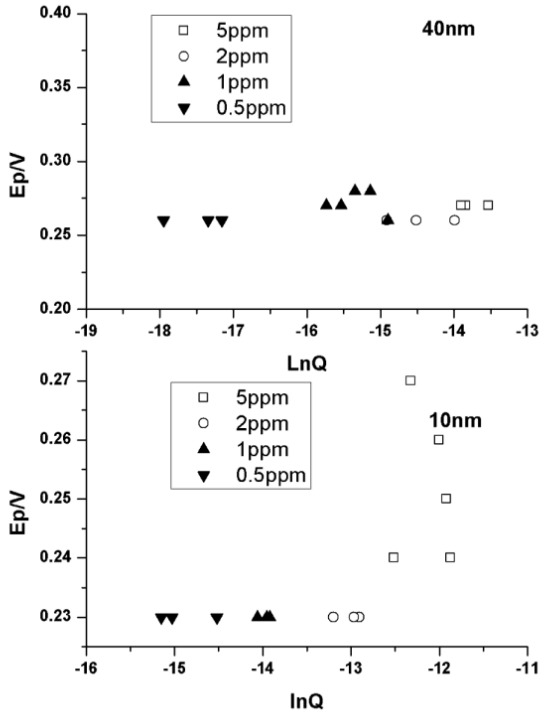

Fig. 2 Influence of the surface coverage on the peak potential. 3 μL of suspensions of different concentrations were deposited on the GC electrode. Three measurements were performed for each concentration.

The slope values obtained using the glassy carbon electrode are 0.054 and 0.066, according to an experiment performed at quite high particle coverage (0.5 mg $L^{-1} = 2 \times 10^{-6}$ mol m^{-2}), small particles (10 to 60 nm) and low scan rates (20 mV s^{-1}).[12,25] The screen printed electrode experiment was performed in duplicate. Linearity was observed from 20 nm to 100 nm. The slopes were different from the GC ones, 0.100 and 0.092, that are consistent with a model of partially overlapping diffusion layers of the deposited NPs. The regression coefficient was in all instances greater than 0.99. Diameter calibration plots and voltammograms obtained using GC and SPEs are shown in Fig. 3.

We consider that the differences between the GC and SPE slopes are due to aggregation of the nanoparticles on the electrode surface during the drying period, which caused the broadening of the peaks and shifting towards more positive potentials, sometimes two peaks could be appreciated clearly[17,26] due to the oxidative dissolution of the AgNP aggregates of different sizes. This problem was minimized by using a convenient dilution and using freshly prepared dilutions every time it was detected. We also noticed that the SPE is prone to this phenomenon, especially with nanoparticles of smaller diameter, probably due to a stronger interaction between the electrode material (because of its chemical composition and surface roughness) and the sample. Examples of multiple peaks for two different nanoparticle diameters are shown in Fig. 4.

Polydispersity not only affects the width of the voltammograms that are broader for SPE than that for GC, but also accounts for the lower values of peak intensity obtained with SPE under the same conditions.[26]

As it can be seen in Table 2, the diameters of the nanoparticles obtained with GC and TEM are similar, but there are some differences when SPEs are used. As a general rule the SPE values are greater than the GC ones, due to the nanoparticle agglomeration on the surface of the SP working electrode.

Concentration of AgNPs in the commercially available colloidal products

Quantitative analysis was performed by studying the relationship between the area under the peak and the concentration of AgNPs in the suspension.

It was found that the slope of the calibration depends on the diameter of the nanoparticles, especially for the screen printed electrode experiments, so it was necessary to use a calibration

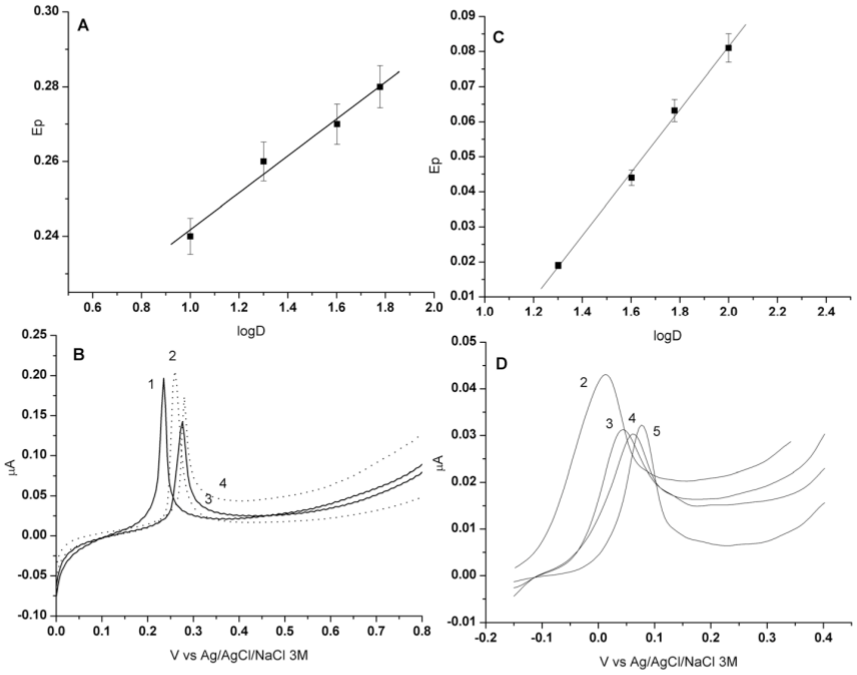

Fig. 3 Diameter calibration plots for GC (A) and SPE (C). Each point is the media of five values. Voltammograms of nanoparticles of different diameters 10 nm (1), 20 nm (2), 40 nm (3), 60 nm (4) and 100 nm (5) for GC (B) and SPE (D).

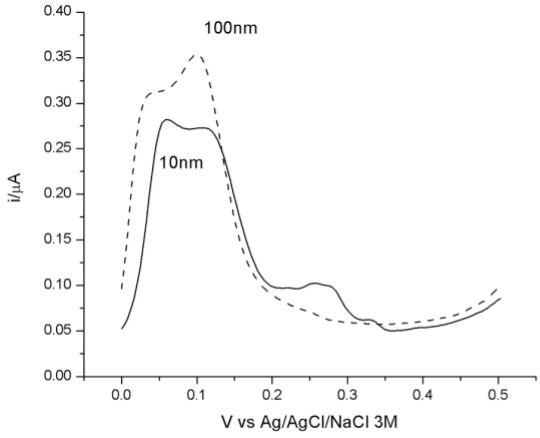

Fig. 4 SPE voltammograms of 5 g mL^{-1} AgNPs (10 nm and 100 nm) showing multiple peaks due to aggregation. 3 μL were deposited on the electrode. Supporting electrolyte 0.1 M $KClO_4$, 70 μL.

with nanoparticle standards close to the diameter of the nanoparticles of the sample. A linear response was obtained from 0.5 mg L^{-1} to 6 mg L^{-1}. Several voltammograms were obtained to be sure that all the nanoparticles were stripped before depositing a second drop of a standard or a sample. It was observed that all of them were oxidized in the first voltammogram. In all instances the regression coefficient was greater than 0.99.

AP10 and AP25 were diluted with Milli Q water five times and SN30 was diluted ten times. 3 μL of the diluted sample were placed on the working electrode, then at least two voltammograms were obtained to be sure that the nanoparticles were totally stripped. Recovery tests were also performed with the glassy carbon electrode and addition of 0.5 mg L^{-1} of the AgNP standard to each sample. The recovery values are 99% for AP10, 95% for AP25 and 110% for SN30. The standard deviation of the recovery values was less than 10%. The quantitative results listed in Table 3 shows that there is good agreement between the experiments. Voltammograms of the samples obtained using GC and the SPE are shown in Fig. 5.

Table 2 AgNP diameter (nm) and peak potential (V) of the particles in silver colloidal products available in the market for health care use. Each value is the mean of two different experiments. Five measurements were performed for each experiment. Results are denoted as mean ± standard deviation

Electrode	AP10 nm V		AP25 nm V		SN30 nm V	
SPE	52 ± 1	0.056 ± 0.003	26 ± 1	0.028 ± 0.003	28 ± 2	0.029 ± 0.004
GC	45 ± 15	0.240 ± 0.025	14 ± 2	0.250 ± 0.010	20 ± 2	0.260 ± 0.005
TEM (nm)	10–50		10–30		20–30	

Table 3 AgNP determination in silver colloidal products. Analyses were performed in duplicate. AgNP diameter of the calibration standards AP10, AP25 40 nm and SN30 20 nm. Results are denoted as mean ± standard deviation

Electrode	AP10 (mg L^{-1})	AP25 (mg L^{-1})	SN30 (mg L^{-1})
SPE	9.65 ± 1.77	5.9 ± 1.37	26.3 ± 2.51
GC	13.2 ± 0.4	4.1 ± 0.2	32.3 ± 0.01
ICP	11.36 ± 0.26	5.34 ± 0.23	23.8 ± 0.80

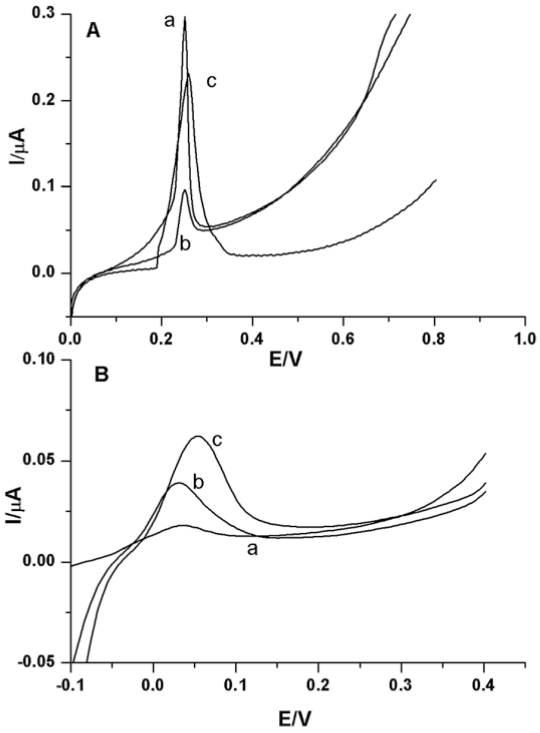

Fig. 5 (A) Voltammograms obtained with GC. 3 μL of the diluted sample deposited on the electrode. (B) SPE voltammograms. 3 μL of the diluted sample cast on the electrode. SN30 (a), AP25 (b) and AP10 (c).

Conclusions

All the samples contained silver nanoparticles mainly in the form of Ag(0). Ag(I) can be detected using CSV, down to 5 μM. In all the samples tested the Ag(I) concentration was lower than 5 μM. Consequently no influence of the Ag(I) concentration on the performance of the reference electrode was considered.

The diameter of the silver nanoparticles can be estimated from the peak potential if the surface coverage is kept constant. If aggregation takes place, two peaks can be observed. The aggregation effect can be minimized by adjusting dilution or preparing a fresh solution for each measurement. 0.5 mg L^{-1} was found to be an adequate concentration for these experiments with AgNPs. It was also noticed that SPEs were prone to cause aggregation of the nanoparticles, which could explain why the diameter values obtained using them are bigger than the ones obtained using GC, but anyway they are within the diameter range observed by TEM.

The concentration of AgNPs in the sample can be determined by anodic stripping voltammetry from a solid deposit of a 3 μL drop of the sample adequately diluted so the ln Q value is lower than −14. In this case, the results obtained with both SPEs and GC electrodes and ICP-MS procedures are in good agreement.

It can be concluded that voltammetry of the immobilized particles on the electrode surface can be used to obtain information about the redox forms present in a commercially available sample of AgNPs as well as the concentration and diameter of the NP. The procedure is quite simple and takes a few minutes. It is of relevance that the SPE is an alternative to the three electrode voltammetric cell since it can offer the same information, opening the door to the development of field sensors for the accurate detection and characterization of nanoparticles, AgNPs in this case.

Acknowledgements

This work has been funded by two projects of "Ministerio de Ciencia e Innovación" "Seribio-biosensores electroquímicos desechables basados en tecnología de serigrafiado" and CTQ2012-38091-C02-01 "Innovaciones en especiación funcional–química en nanotecnología medioambiental (Nanometrología). Caracterización de nanopartículas artificiales y materia orgánica natural".

Notes and references

1 C. R. Thomas, S. George, A. M. Horst, Z. Ji, R. J. Miller, J. R. Peralta-Videa, T. Xia, S. Pokhrel, L. Mädler, J. L. Gardea-Torresdey, P. A. Holden, A. A. Keller, H. S. Lenihan, A. E. Nel and J. I. Zink, *ACS Nano*, 2011, **5**, 13.
2 C. Carlson, S. M. Hussain, A. M. Schrand, L. K. Braydich-Stolle, K. L. Hess, R. L. Jones and J. J. Schlager, *J. Phys. Chem. B*, 2008, **112**, 13608.
3 M. Hassellöv, J. W. Readman, J. F. Ranville and K. Tiede, *Ecotoxicology*, 2008, **17**, 344.
4 J. Gigault, J. M. Pettibone, C. Schmitt and V. A. Hackley, *Anal. Chim. Acta*, 2014, **809**, 9.
5 E. Bolea, J. Jiménez-Lamana, F. Laborda and J. R. Castillo, *Anal. Bioanal. Chem.*, 2011, **401**, 2723.
6 F. Laborda, J. Jiménez-Lamana, E. Bolea and J. R. Castillo, *J. Anal. At. Spectrom.*, 2013, **28**, 1220.
7 Y. G. Zhou, N. V. Rees and R. G. Compton, *Angew. Chem., Int. Ed.*, 2011, **50**, 4219.
8 N. V. Rees, Y. G. Zhou and R. G. Compton, *ChemPhysChem*, 2011, **12**, 1645.
9 E. J. E. Stuart, N. V. Rees, J. T. Cullen and R. G. Compton, *Nanoscale*, 2013, **5**, 174.
10 Y. G. Zhou, N. V. Rees, J. Pillay, R. Tshikhudo, S. Vilakazi and R. G. Compton, *Chem. Commun.*, 2012, **48**, 224.
11 F. Scholz and B. Meyer, *Electroanal. Chem.*, 1996, **20**, 1.
12 S. E. Ward Jones, F. W. Campbell, R. Baron, L. Xiao and R. G. Compton, *J. Phys. Chem. C*, 2008, **112**, 1780.

13 K. Z. Brainina, L. G. Galperin and A. L. Galperin, *J. Solid State Electrochem.*, 2010, **14**, 981.
14 K. Z. Brainina, L. G. Galperin, T. Y. Kiryuhina, A. L. Galperin, N. Y. Stozhko, A. M. Murzakaev and O. R. Timoshenkova, *J. Solid State Electrochem.*, 2012, **16**, 2365.
15 W. J. Plieth, *J. Phys. Chem.*, 1982, **86**, 3166.
16 K. Z. Brainina, L. G. Galperin and E. V. Vikulova, *J. Solid State Electrochem.*, 2012, **16**, 2357.
17 H. S. Toh, C. McAuley, K. Tschulik, M. Uhlemann, A. Crossley and R. G. Compton, *Nanoscale*, 2013, **5**, 4884.
18 I. Shitanda, H. Kiryu and M. Itagaki, *Electrochim. Acta*, 2011, **58**, 528.
19 W. Y. Liao and T. C. Chou, *Anal. Chem.*, 2006, **78**, 4219.
20 D. Cicmil, S. Anastasova, A. Kavanagh, D. Diamond, U. Mattinen and J. Bobacka, *Electroanalysis*, 2011, **23**, 1881.
21 D. Desmond, B. Lane, J. Alderman, J. D. Glennon and D. Diamond, *Sens. Actuators, B*, 1997, **44**, 389.
22 M. A. Nolan, S. H. Tan and S. P. Kounaves, *Anal. Chem.*, 1997, **69**, 1244.
23 E. J. E. Stuart, K. Tschulik, D. Omanovic, J. T. Cullen, K. Jurkschat, A. Crossley and R. G. Compton, *Nanotechnology*, 2013, DOI: 10.1088/0957–4484/24/44/444002.
24 K. Tschulik, R. G. Palgrave, C. Batchelor-McAuley and R. G. Compton, *Nanotechnology*, 2013, DOI: 10.1088/0957-4484/24/29/295502.
25 S. E. Ward Jones, F. G. Chevallier, C. A. Paddon and R. G. Compton, *Anal. Chem.*, 2007, **79**, 4110.
26 K. Z. Brainina, L. G. Galperin, E. V. Vikulova and A. L. Galperin, *J. Solid State Electrochem.*, 2013, **17**, 43.

A1 *Samples of AgNPs on Glassy Carbon electrode (GC).*

Graph and results released from the voltammograms subjected to deconvolution.

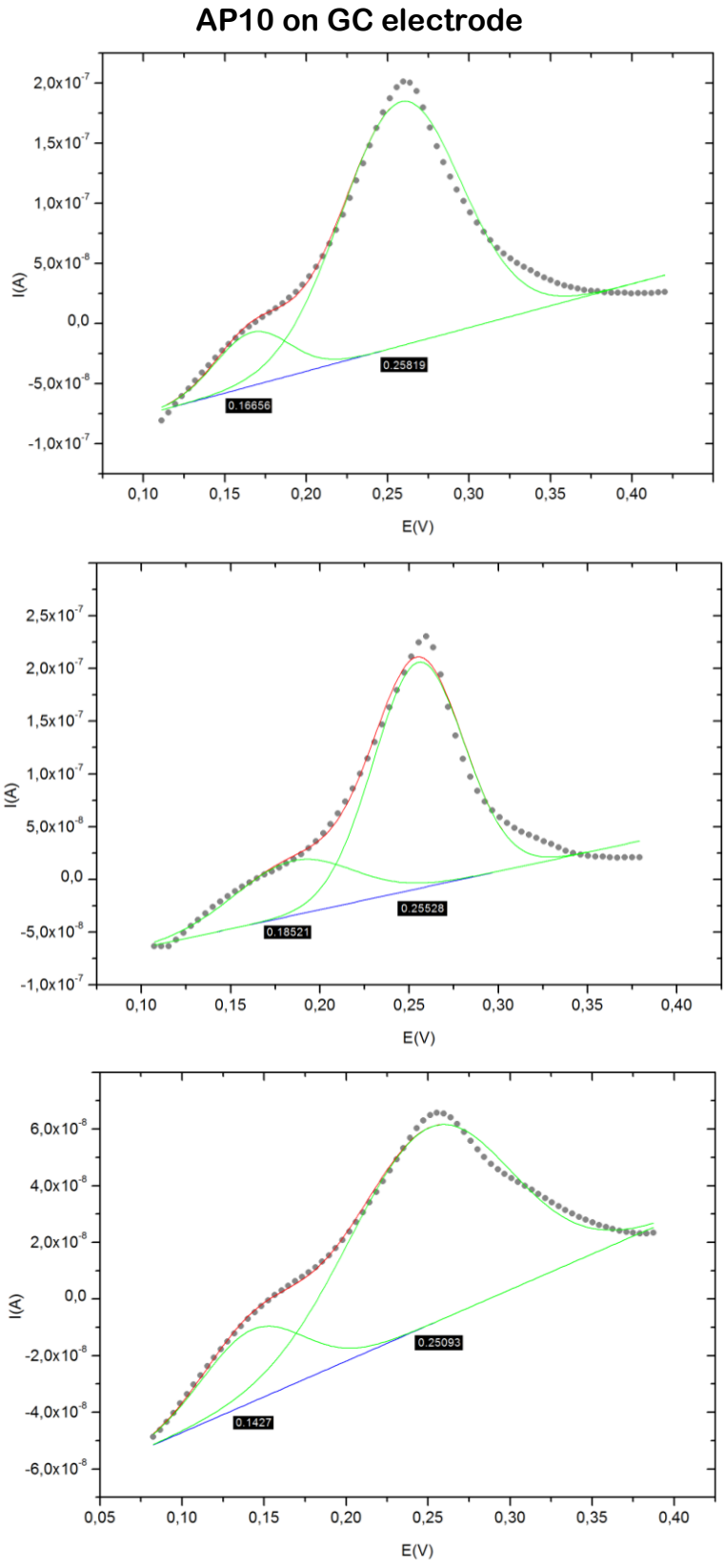

AP25 on GC electrode

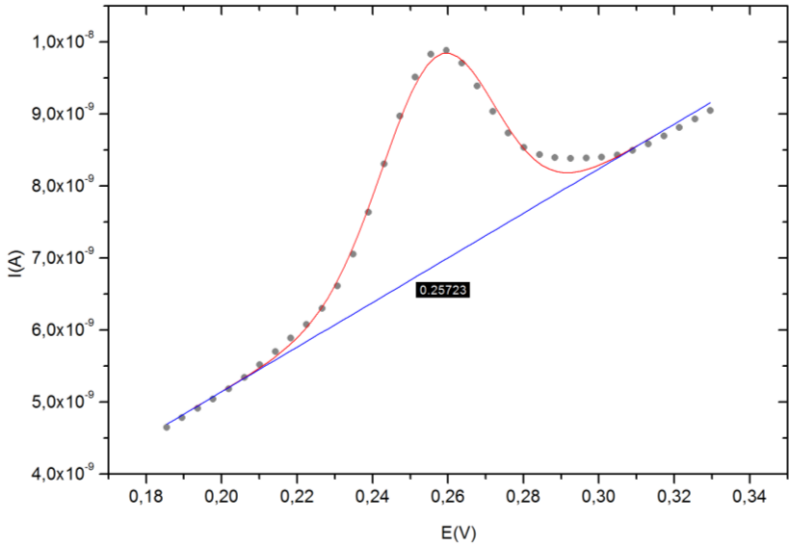

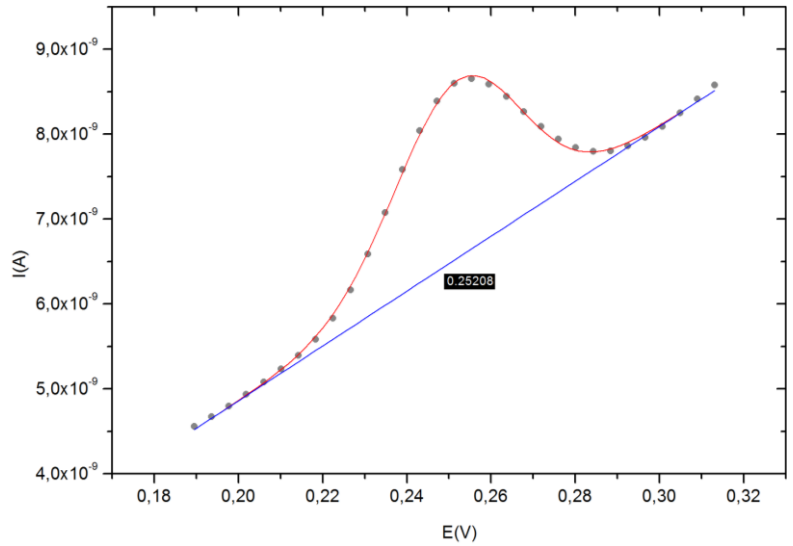

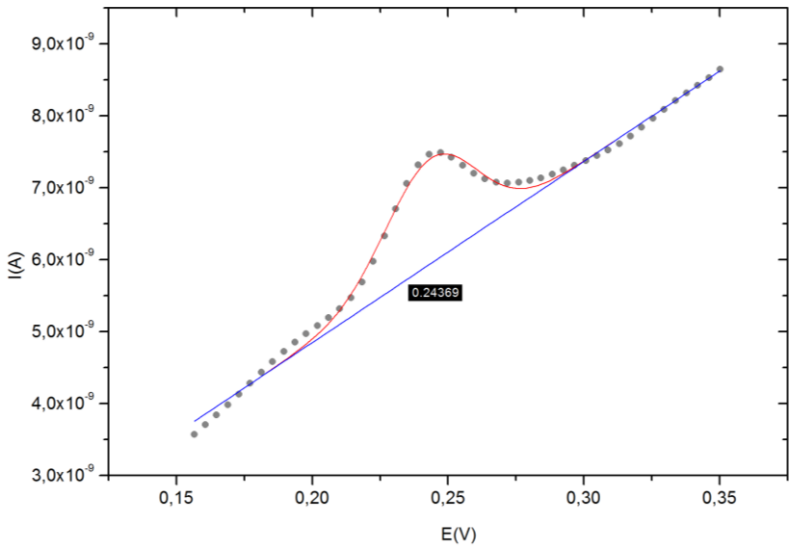

SN30 on GC electrode

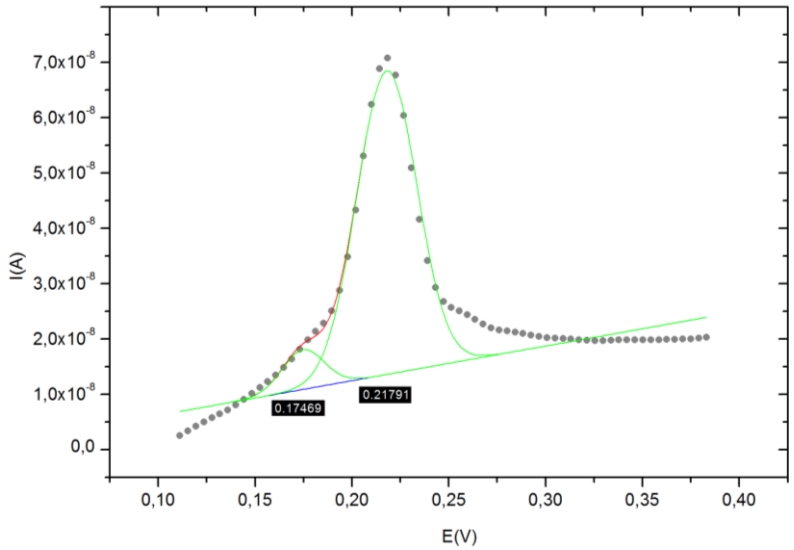

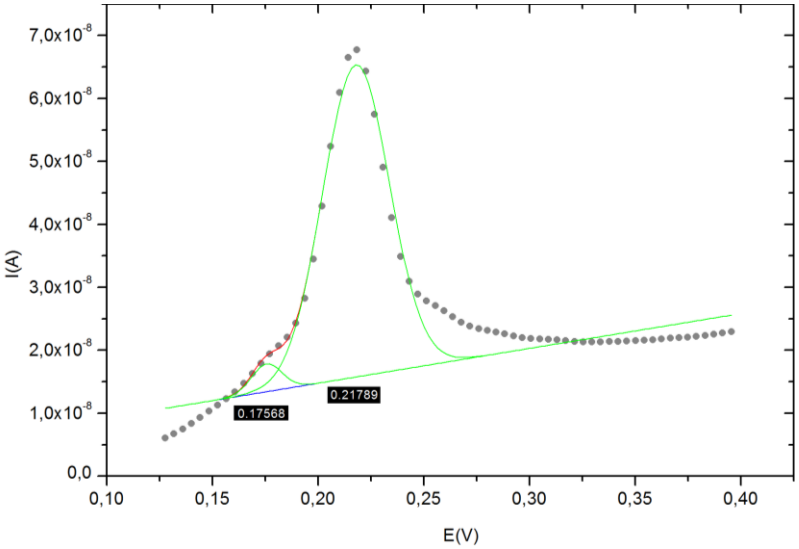

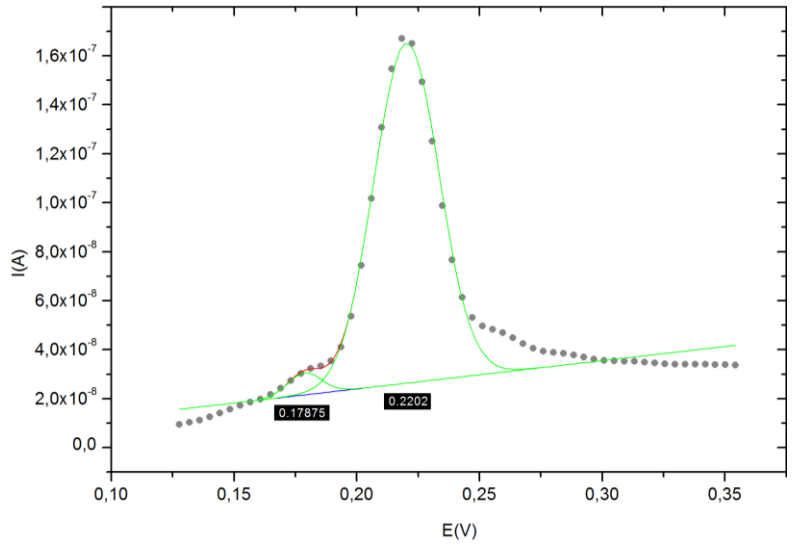

A2 *Samples of AgNPs on a modified Screen Printed Carbon Electrode (SPCE).* Graph and results released from the voltammograms subjected to deconvolution.

AP10 on modified SPCE

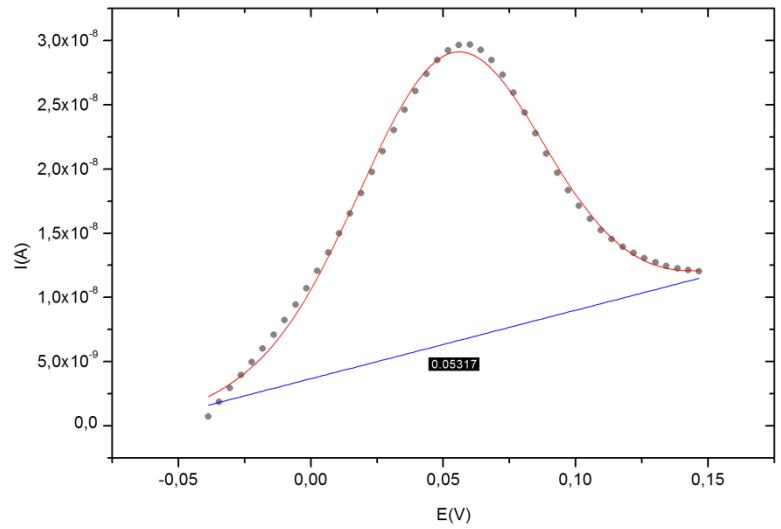

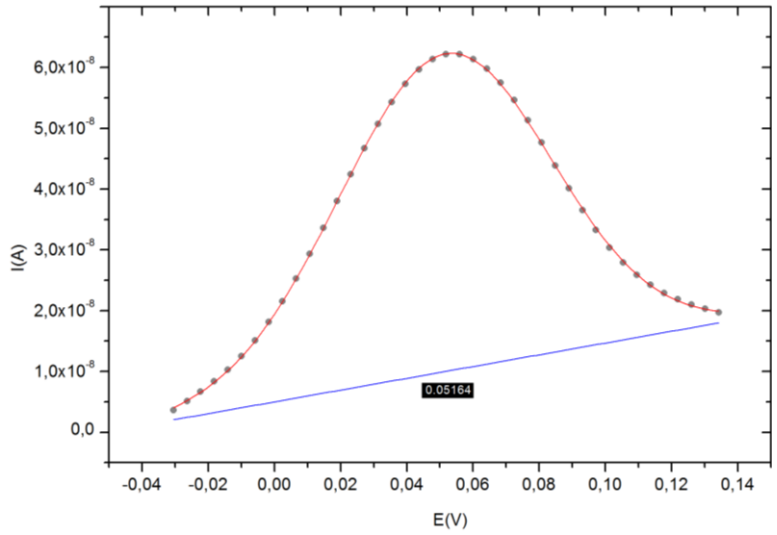

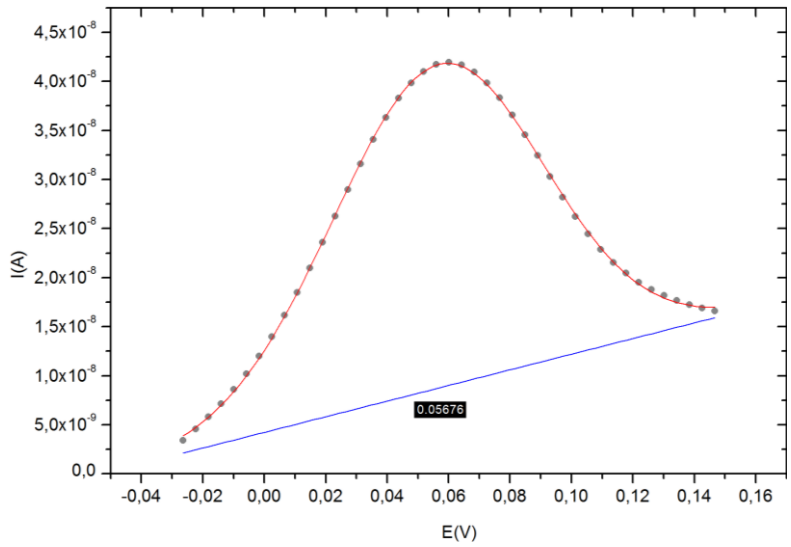

AP25 on modified SPCE

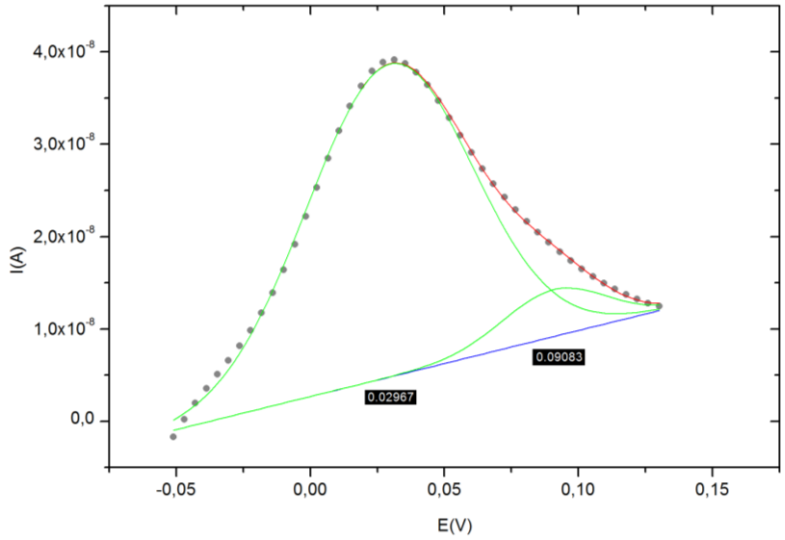

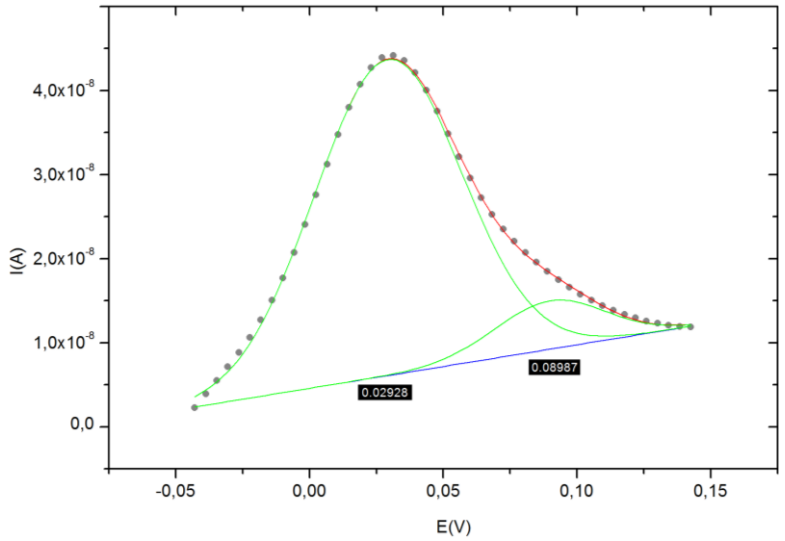

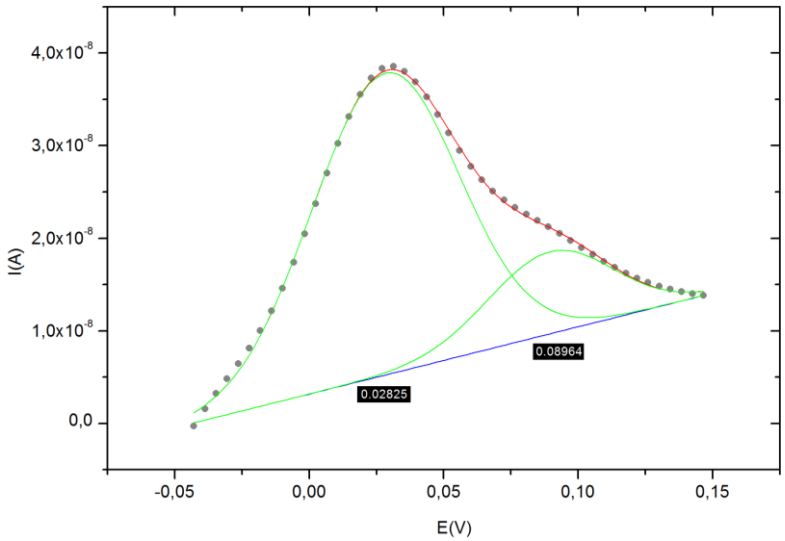

SN30 on modified SPCE

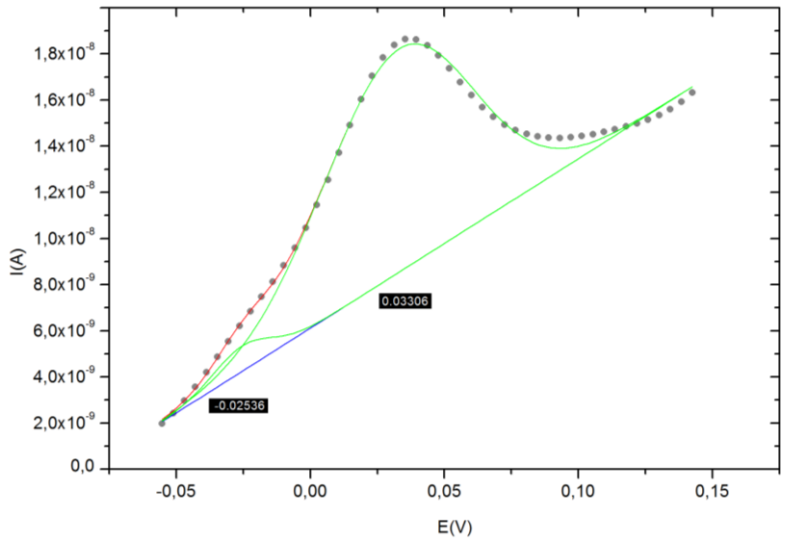

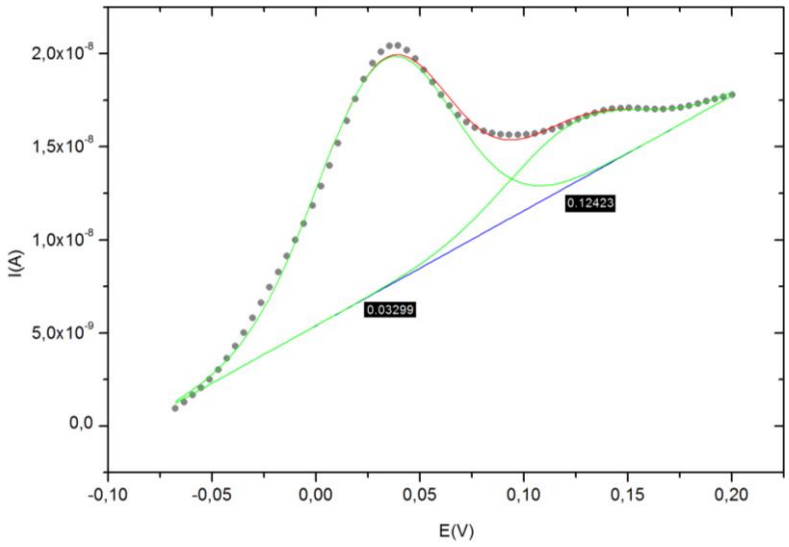

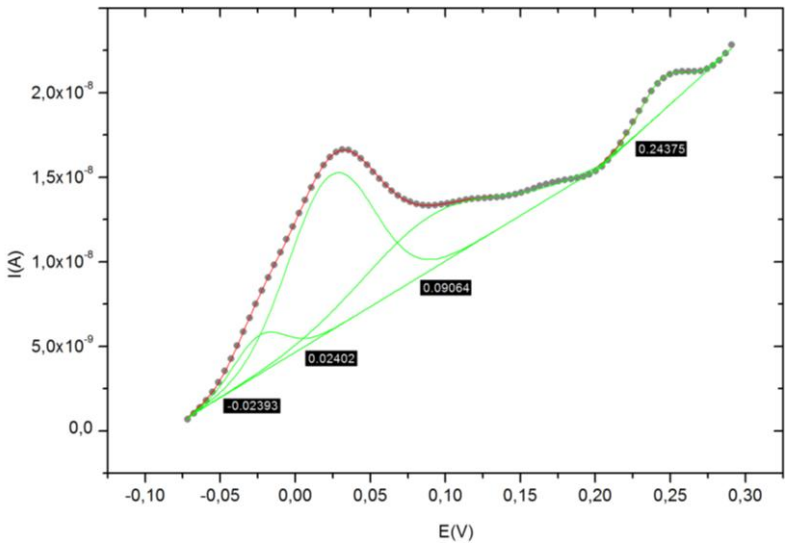

A3 *Photograph of the electrodes used in Particle Collision.*

(1) is reference electrode of Ag/AgCl/3M NaCl, (2) is Glassy Carbon microelectrode (GC-ME) with 11 ± 2µm of diameter, (3) is Platinum microelectrode (Pt-ME) with 10µm of diameter and (4) is Pt wire as auxiliary electrode.

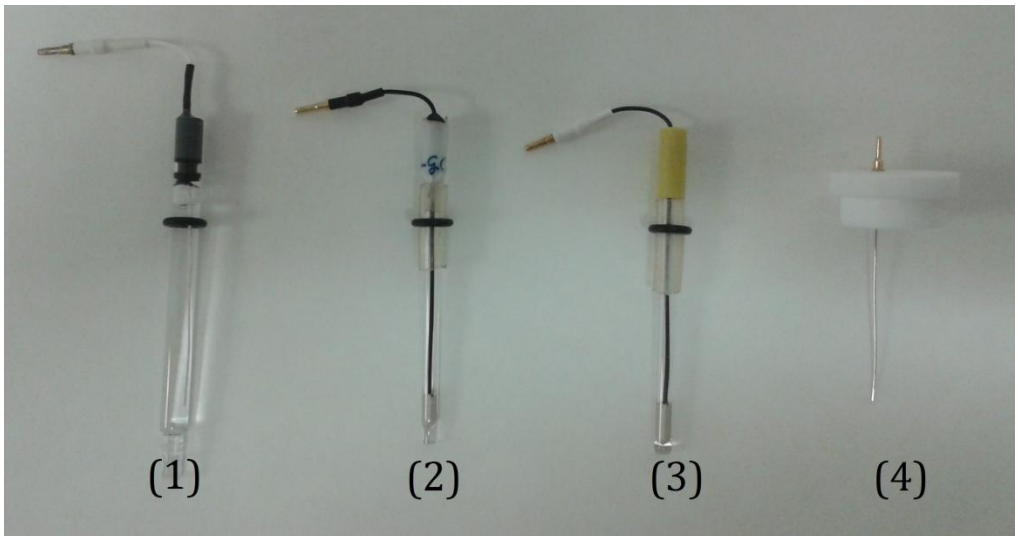

A4 Study of silver nanoparticles (AgNPs) by Direct Particle Collision.

The procedures, parameters or features used are described in this annex.

i) 10mL of 10mM citrate† and 90mM NaCl as supporting electrolyte. Solution of AgNPs 100nm was used. The measurements parameters are:

E (V)	Measurement duration (s)	Measuring time (s)
0,5	10	0,001
0,5	5	0,0005

The concentration of AgNPs in 10mL of electrolyte was $2{,}73.10^{13}$NP L^{-1}. Twenty measurements of 10s and twenty measurements of 5s were saved but without results.

ii) A second experiment was performed with the same parameters of the previous experiment but the twice of AgNPs (100nm) were injected into the cell. The concentration of AgNPs in 10mL of electrolyte was $5{,}46.10^{13}$NP L^{-1}. Twenty measurements of 10s and twenty measurements of 5s were saved but neither show results.

iii) In this experiment, we tried to increase the number of NPs per liter to 10^{16} and the measurement parameters were the same. Twenty measurements of 10s and twenty measurements of 5s were saved but neither show results.

iv) The supporting electrolyte was changed (90mM NaCl was changed by 90mM $NaClO_4$) because Cl^- can acts as glue and aggregate the AgNPs. Six experiments were performed with the new electrolyte. Ten measurements of 10s and ten measurements of 5s were saved but neither show results.

v) With these parameters and last electrolyte, other test were performed with standards of 10nm ($1{,}83.10^{16}$NP L^{-1} - 0,1ppm) and 40nm ($5{,}68.10^{13}$NP L^{-1} – 0,02ppm). Sixty measurements of 10s and sixty measurements of 5s were saved and not gave results for AgNPs 10nm. Twenty measurements of 10s and twenty measurements of 5s were saved but neither show results for AgNPs 40nm.

In direct approach, any procedure used gave valid results.

†Citrate is a compound that easily deteriorates, therefore, must be prepared at the time of use in each experiment.

A5 Study of silver nanoparticles (AgNPs) by Electrocatalytic Particle Collision.

The procedures, parameters or features used are described in this annex.

i) 10mL of 0,1M $NaClO_4$ and 2,8mM H_2O_2 as supporting electrolyte. Solution of AgNPs 100nm was used. The measurements parameters are:

E (V)	Measurement duration (s)	Measuring time (s)
-0,9	10	0,001
-0,9	5	0,0005

The concentration of AgNPs in 10mL of electrolyte was $2{,}73.10^{13}$NP L^{-1}. Twenty measurements of 10s and twenty measurements of 5s were saved. **This procedure gave valid results for measurements of 10s (Two peaks were extracted).**

ii) The same above experiment was repeated without success. Then, the experiment was repeated injecting a double volume of AgNPs (100nm). The concentration of AgNPs in 10mL of electrolyte was $5{,}46.10^{13}$NP L^{-1}. Ten measurements of 10s and ten measurements of 5s were saved but not collision events were detected.

iii) Another solution was tried. The sample SN30 undiluted was injected and neither obtains results. The concentration of AgNPs (SN30) in 10mL of electrolyte was $3{,}03.10^{14}$NP L^{-1}. Ten measurements of 10s and ten measurements of 5s were saved but not gave results.

iv) One ($3{,}03.10^{14}$NP L^{-1}), two ($6{,}06.10^{14}$NP L^{-1}) and three ($9{,}09.10^{14}$NP L^{-1}) volumes of SN30 sample in three different experiments with the electrolyte without hydrogen peroxide (no electrocatalytic) were also tested. The parameters were the same. Twenty measurements of 10s in each experiment were saved and any of them gave collision events.

v) 10mL of 0,1M $NaClO_4$ and 10mM citrate (without H_2O_2) as electrolyte. The concentration of AgNPs 100nm in 10mL of electrolyte was $2{,}73.10^{13}$NP L^{-1}. The same parameters were used. Twenty measurements of 10s were saved but not collision events were observed.

vi) 10mL of 0,1M $NaClO_4$, 10mM citrate and 2,8mM H_2O_2 as electrolyte. The concentration of AgNPs 100nm in 10mL of electrolyte was $2{,}73.10^{13}$NP L^{-1}. The same parameters were used. Twenty measurements of 10s were saved but not collision events were observed.

vii) 10mL of 0,1M $NaClO_4$, 10mM citrate and 4,9mM H_2O_2 as electrolyte. The concentration of AgNPs 100nm in 10mL of electrolyte was $2{,}73.10^{13}$NP L^{-1}. The same parameters were used. Twenty measurements of 10s were saved but neither collision events were observed.

A6 Study of ceria nanoparticles (CeO_2NPs or nanoceria) by Direct Particle Collision (PC).

The procedures, parameters or features used or tested are described in this annex.

i) 10mL of 1M HCl is used as supporting electrolyte. GC-ME and Pt-ME are used as WE. The measurements parameters are:

E (V)	Measurement duration (s)	Measuring time (s)
0	10	0,001

The concentration of 4nm nanoceria in 10mL of electrolyte was 5000ppm ($1{,}95.10^{19}$NP L^{-1}). Twenty measurements with GC-ME and twenty measurements with Pt-ME were collected but without results.

ii) 10mL of 1M HCl is used as supporting electrolyte. GC-ME is used as WE. The measurements parameters are:

E (V)	Measurement duration (s)	Measuring time (s)
-0,5	10	0,001

The concentration of 4nm nanoceria in 10mL of electrolyte was 1000ppm ($3{,}9.10^{18}$NP L^{-1}). **Fifty-two measurements were saved with valid results (43 peaks were extracted).**

iii) In order to obtain the same results as in A6ii, the last experience with the same parameters was repeated. One hundred ten measurements were obtained in three repetitions but any result was obtained.

iv) The same conditions and parameters were used with 10-20nm nanoceria. The concentration of 10-20nm nanoceria in 10mL of electrolyte was 1000ppm ($3{,}12.10^{16}$NP L^{-1}). One hundred measurements were saved in two different experiences but no collision events were detected.

v) Valid procedure (A6ii) was tested with standard of 10-20nm nanoceria. The concentration of 10-20nm nanoceria in 10mL of electrolyte was 1410ppm ($3{,}86.10^{18}$NP L^{-1}). Twenty measurements were saved in two different experiences but without collision events.

A7 Study of nanoceria by catalytic reduction particle collision.

The procedures, parameters or features used are described in this annex.

i) 10mL of 1M HCl and 10mM H_2O_2 is used as supporting electrolyte. GC-ME and Pt-ME are used as WE. The measurements parameters are:

E (V)	Measurement duration (s)	Measuring time (s)
0	10	0,001

The concentration of 4nm nanoceria in 10mL of electrolyte was 5000ppm ($1,95.10^{19}$NP L^{-1}). Twenty measurements with GC-ME and twenty measurements with Pt-ME were saved but without results.

ii) 10mL of 1M HCl and 10mM H_2O_2 is used as supporting electrolyte. GC-ME is used as WE. The measurements parameters are:

E (V)	Measurement duration (s)	Measuring time (s)
-0,5	10	0,001

The concentration of 4nm nanoceria in 10mL of electrolyte was 1000ppm ($3,9.10^{18}$NP L^{-1}). Thirty-five measurements were saved but without results.

iii) 10mL of 1M HCl and 10mM H_2O_2 is used as supporting electrolyte. Pt-ME is used as WE. H_2O_2 and nanoceria were in contact for 1½ hours before measuring. The measurements parameters are:

E (V)	Measurement duration (s)	Measuring time (s)
-0,2	10	0,001

The concentration of 4nm nanoceria in 10mL of electrolyte was 990ppm ($3,86.10^{18}$NP L^{-1}). Pt-ME was immersed in 10mM $NaBH_4$ solution for 15 minutes just before measuring (Activation of WE). **One hundred measurements were saved with valid results (285 peaks were extracted).**

iv) The same conditions and parameters were used with 10-20nm nanoceria. The concentration of 10-20nm nanoceria in 10mL of electrolyte was 1000ppm ($3,12.10^{16}$NP L^{-1}). One hundred measurements were saved in two different experiences but no collision events were observed.

v) 10mL of 2,5% acetic acid is used as supporting electrolyte because the 10-20nm nanoceria are suspended in this electrolyte. The others conditions and parameters were the same. Concentration was increased to increase the probability of observing a collision event. The concentration of 10-20nm nanoceria in 10mL of electrolyte was 5000ppm ($1,56.10^{17}$NP L^{-1}). One hundred measurements were saved in two different experiences but without results.

vi) 5mL of 0,1M HCl and 20mM H_2O_2 is used as supporting electrolyte. Pt-ME is used as WE. H_2O_2 and nanoceria were in contact for 1 hour. The measurements parameters are the same that the valid procedure (A7iii). The concentration of 10-20nm nanoceria in 5mL of electrolyte was

1410ppm ($3{,}86.10^{18}$NP L^{-1}). Twenty measurements were saved but without results.

vii) 5mL of 1M HCl and 20mM H_2O_2 is used as supporting electrolyte. Pt-ME is used as WE. H_2O_2 and nanoceria were in contact for 30 minutes. The measurements parameters are the same that the valid procedure (A7iii). The concentration of 4nm nanoceria in 5mL of electrolyte was 1890ppm ($7{,}37.10^{18}$NP L^{-1}). Pt-ME was activated with the same previous procedure. Forty measurements were saved in two different experiences but just one peak was observed. The procedure is not useful.

viii) In this case, we followed the procedure of reference [50] which indicates the use of centrifuge to remove excess of hydrogen peroxide. 5mL of 0,1M HCl and 10mM H_2O_2 is used as supporting electrolyte. Pt-ME is used as WE. H_2O_2 and nanoceria were in contact for 30 minutes. After this time, 7-10mL of 3M NaCl are added to precipitate nanoceria. To remove the excess of H_2O_2, the solution was centrifuged (5000rpm for 10 minutes), supernatant is discarded, add 5mL of 0,1M HCl and again centrifuged, supernatant is discarded and finally the nanoceria are redispersed in 5mL of 0,1M HCl to measure. The measurements parameters are the same that the valid procedure (A7iii). The concentration of 4nm nanoceria in 5mL of electrolyte was 1890ppm ($7{,}37.10^{18}$NP L^{-1}). Pt-ME was activated with the same previous procedure. Forty measurements were saved in two different experiences but just one peak was observed. The procedure is not useful.

ix) Latter procedure was repeated but nanoceria concentration was changed. The concentration of 4nm nanoceria in 5mL of electrolyte was 990ppm ($3{,}86.10^{18}$NP L^{-1}). The measurements parameters are the same that the valid procedure (A7iii). Twenty measurements were saved but without results.

x) In this procedure, we look a new redox reaction and tried with hydrogen and sodium borohydride. Hydrogen is obtained "in situ" by the reaction between $NaBH_4$ and acid media ($BH_4^- + H^+ + 3H_2O \rightarrow H_3BO_3 + 4H_2$). H_2 is conduced to the cell with nitrogen and it is bubbled on the nanoceria solution. 0,4372g of $NaBH_4$ in 30mL of 0,1M HCl is used as source of hydrogen. The measurements parameters are the same that the valid procedure (A7iii). Twenty measurements were saved but without results.

xi) Another way to reduce nanoceria is the direct use of $NaBH_4$. $NaBH_4$ is a strong reducing agent and the reduction can be excessive. 5mL of 0,1M HCl is the electrolyte. Pt-ME is used as WE. The concentration of 4nm nanoceria in 5mL of electrolyte was 1410ppm ($5{,}5.10^{18}$NP L^{-1}). 0,2mg of $NaBH_4$ is added on the cell. $NaBH_4$ and nanoceria were in contact for 30 minutes and then nitrogen is bubbled to displace the excess of hydrogen. WE is chemically activated as the previous cases. **Thirty measurements were saved with the same parameters that A7iii (11 peaks were observed).**

xii) 5mL of 0,1M HCl is the electrolyte. Pt-ME is used as WE. The parameters used were:

E (V)	Measurement duration (s)	Measuring time (s)
-0,2	20	0,002

The concentration of 10-20nm nanoceria in 5mL of electrolyte was 1410ppm ($3{,}86.10^{18}$NP L^{-1}). 0,2mg of $NaBH_4$ is added on the cell. $NaBH_4$ and nanoceria were in contact for 30-60 minutes and then nitrogen is bubbled to displace the excess of hydrogen. WE is chemically activated as the previous cases. **Thirty-three measurements were saved with valid results (53 peaks were extracted).**

xiii) The above procedure (xii) is repeated for 10-20nm nanoceria with the same parameters and features. **One hundred ninety measurements were saved with valid results (10 peaks were extracted).**

A8 Plots of peaks in 4nm nanoceria by direct PC.

Some peaks obtained by direct PC following the general procedure and parameters collected in A6ii are shown. Eight graphics with peaks were superimposed in each plot.

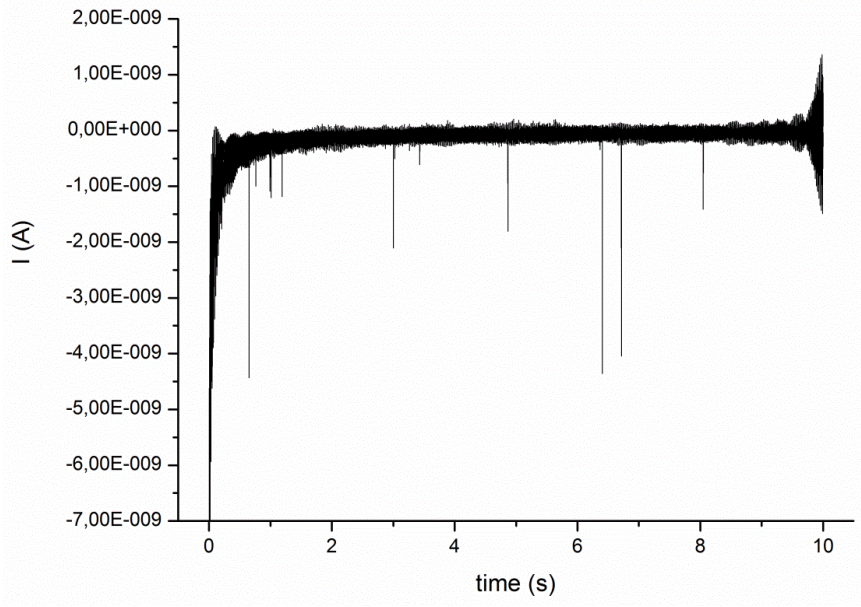

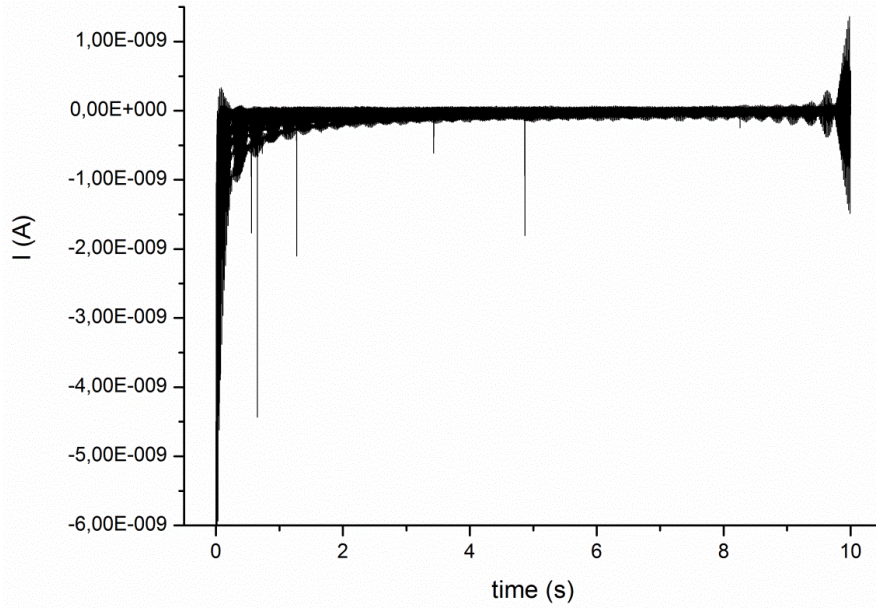

A9 Plots of peaks in 4nm nanoceria by catalytic reduction particle collision.

Some peaks obtained by direct modified PC following the general procedure and parameters collected in A7iii are shown. Thirteen graphics with peaks were superimposed in all plots.

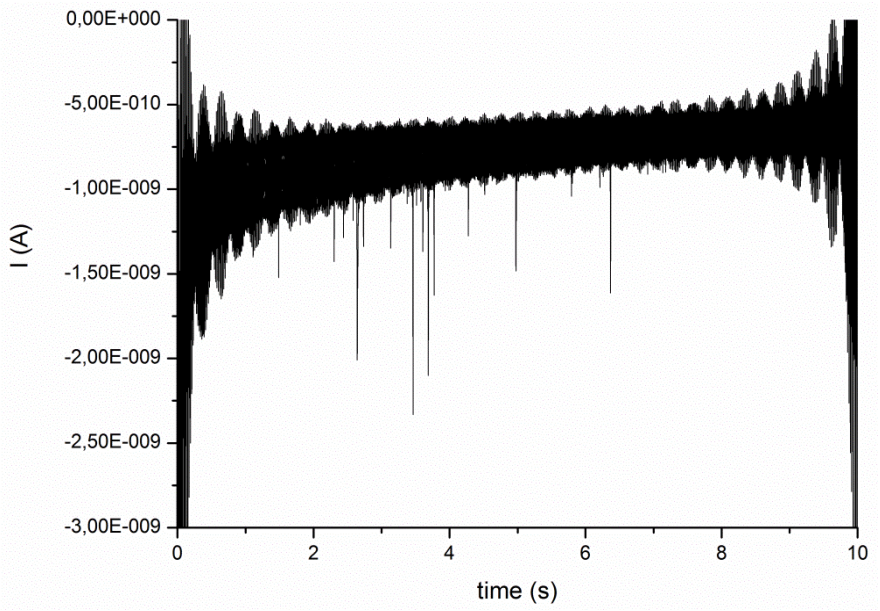

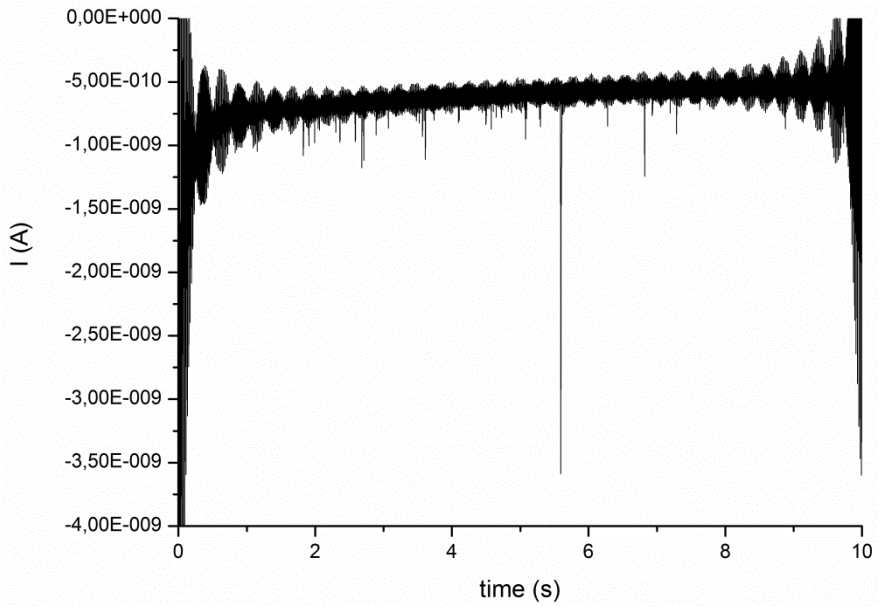

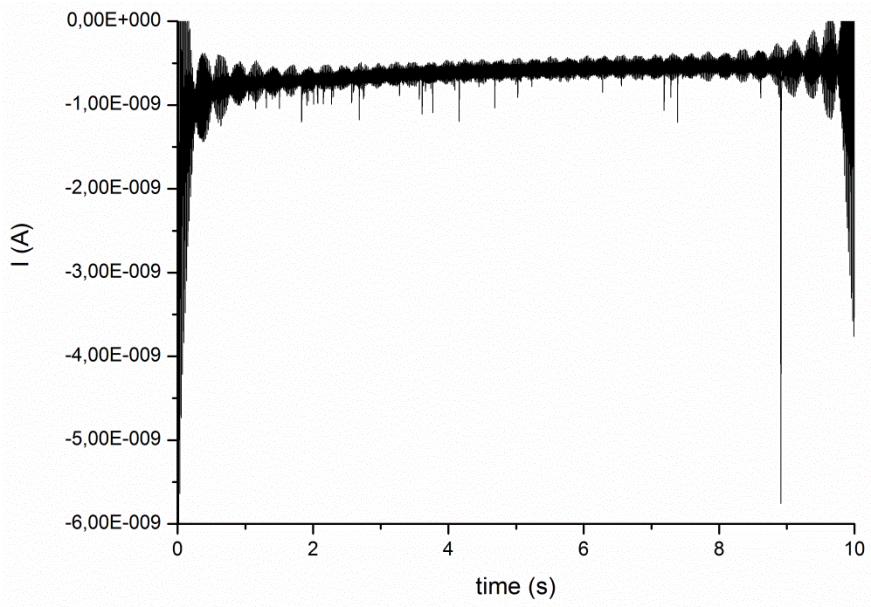
0,00E+000
-1,00E-009
-2,00E-009
-3,00E-009
-4,00E-009
-5,00E-009
-6,00E-009
I (A)
0
2
4
6
8
10
time (s)

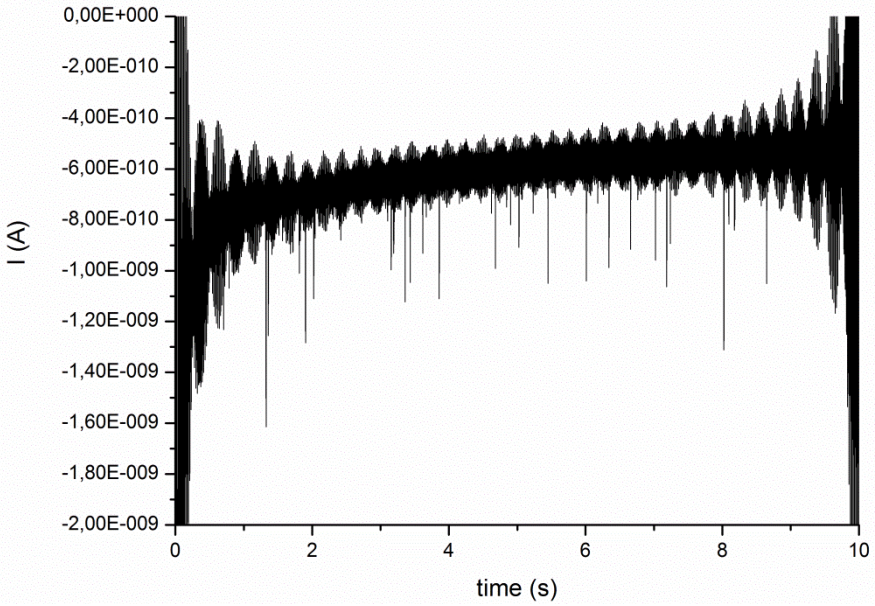
0,00E+000
-2,00E-010
-4,00E-010
-6,00E-010
-8,00E-010
-1,00E-009
-1,20E-009
-1,40E-009
-1,60E-009
-1,80E-009
-2,00E-009
I (A)
0
2
4
6
8
10
time (s)

A10 Radii of 4nm nanoceria by catalytic reduction particle collision.

Radii obtained following the general procedure and parameters collected in A7iii

Nº of peaks	**r (nm)**	**Nº of peaks**	**r (nm)**	**Nº of peaks**	**r (nm)**	**Nº of peaks**	**r (nm)**
1	5	40	20	79	4	118	2
2	2	41	3	80	3	119	4
3	5	42	3	81	2	120	2
4	4	43	4	82	6	121	3
5	6	44	3	83	5	122	4
6	2	45	5	84	6	123	3
7	3	46	21	85	4	124	4
8	7	47	2	86	6	125	3
9	3	48	5	87	5	126	1
10	1	49	3	88	3	127	3
11	2	50	3	89	2	128	5
12	8	51	3	90	4	129	6
13	2	52	2	91	4	130	4
14	10	53	5	92	4	131	4
15	4	54	5	93	4	132	5
16	3	55	4	94	2	133	2
17	5	56	5	95	4	134	8
18	2	57	3	96	2	135	4
19	3	58	3	97	3	136	5
20	3	59	2	98	2	137	3
21	3	60	3	99	3	138	4
22	2	61	3	100	2	139	6
23	3	62	6	101	4	140	3
24	3	63	10	102	10	141	5
25	3	64	5	103	5	142	2
26	2	65	3	104	5	143	4
27	3	66	11	105	6	144	5
28	3	67	6	106	3	145	4
29	2	68	5	107	4	146	3
30	5	69	2	108	66	147	3
31	4	70	7	109	3	148	1
32	2	71	20	110	3	149	2
33	2	72	5	111	3	150	5
34	3	73	10	112	3	151	3
35	4	74	8	113	5	152	6
36	4	75	5	114	2	153	3
37	2	76	4	115	2	154	3
38	17	77	7	116	2	155	5
39	9	78	2	117	3	156	1

Nº of peaks	r (nm)	Nº of peaks	r (nm)	Nº of peaks	r (nm)	Nº of peaks	r (nm)
157	2	199	8	241	6	283	3
158	2	200	5	242	2	284	6
159	2	201	4	243	4	285	6
160	3	202	4	244	3		
161	5	203	3	245	3		
162	6	204	2	246	1		
163	4	205	11	247	2		
164	6	206	4	248	8		
165	4	207	3	249	3		
166	44	208	5	250	2		
167	3	209	7	251	2		
168	4	210	3	252	10		
169	2	211	2	253	4		
170	5	212	2	254	2		
171	3	213	9	255	3		
172	2	214	2	256	2		
173	39	215	3	257	7		
174	5	216	3	258	4		
175	4	217	8	259	10		
176	4	218	2	260	2		
177	6	219	2	261	4		
178	3	220	5	262	10		
179	13	221	6	263	5		
180	2	222	2	264	6		
181	2	223	3	265	11		
182	4	224	5	266	9		
183	3	225	2	267	2		
184	3	226	7	268	4		
185	3	227	3	269	2		
186	4	228	6	270	3		
187	5	229	3	271	6		
188	3	230	2	272	4		
189	5	231	2	273	5		
190	2	232	3	274	10		
191	6	233	4	275	3		
192	5	234	5	276	8		
193	6	235	4	277	10		
194	4	236	6	278	5		
195	2	237	6	279	19		
196	3	238	2	280	2		
197	3	239	2	281	5		
198	2	240	2	282	3		

A11 UV spectra of 10-20nm nanoceria with 1, 2, 4, 6 and 8mM Ascorbic Acid (AA).

The spectra measured of each AA concentration to intervals of 5 minutes are shown below.

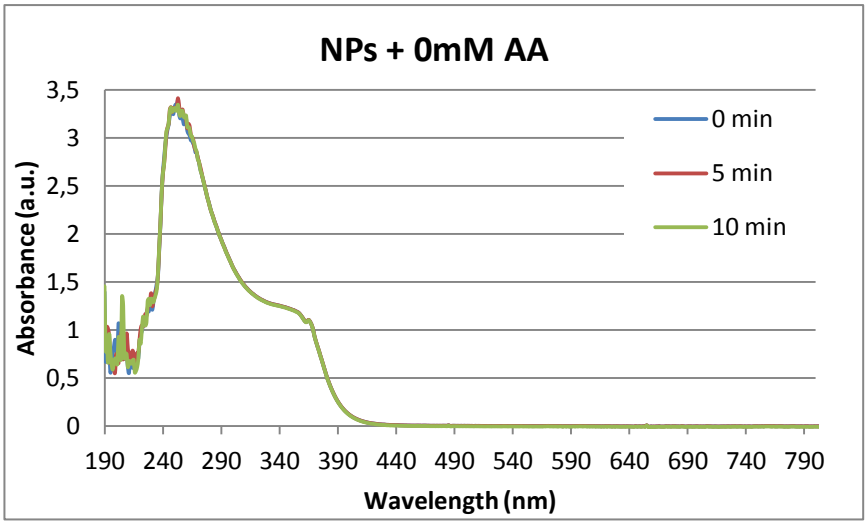

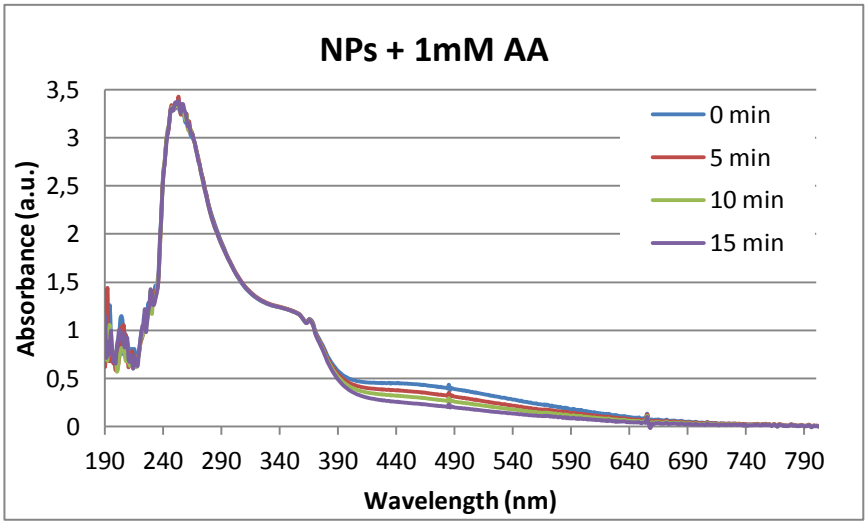

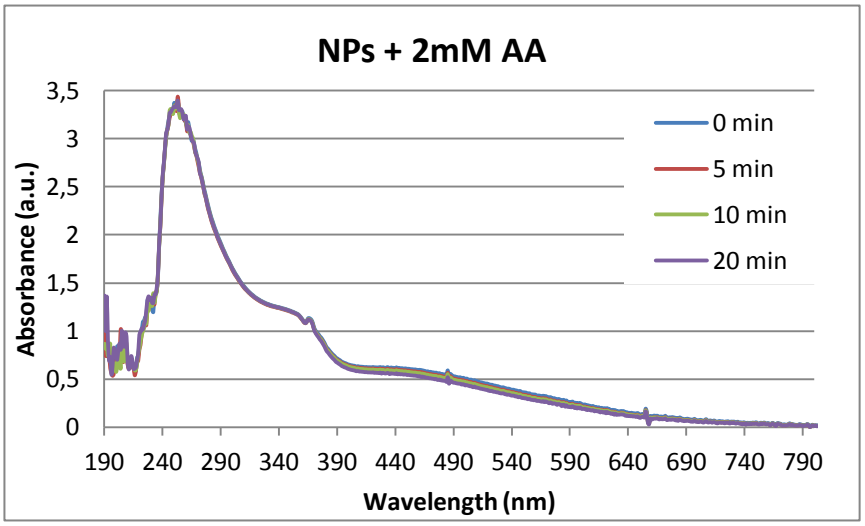

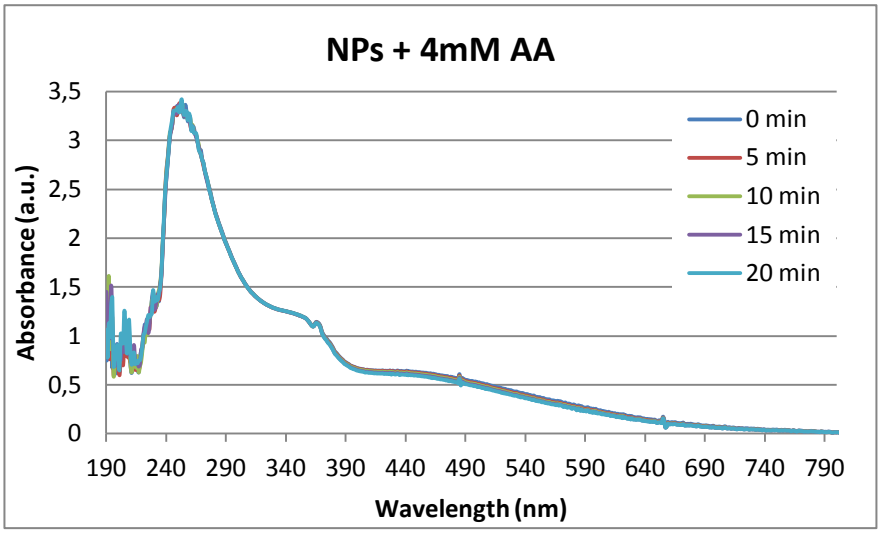
NPs + 4mM AA
Absorbance (a.u.)
3,5
3
2,5
2
1,5
1
0,5
0
190 240 290 340 390 440 490 540 590 640 690 740 790
Wavelength (nm)
0 min
5 min
10 min
15 min
20 min

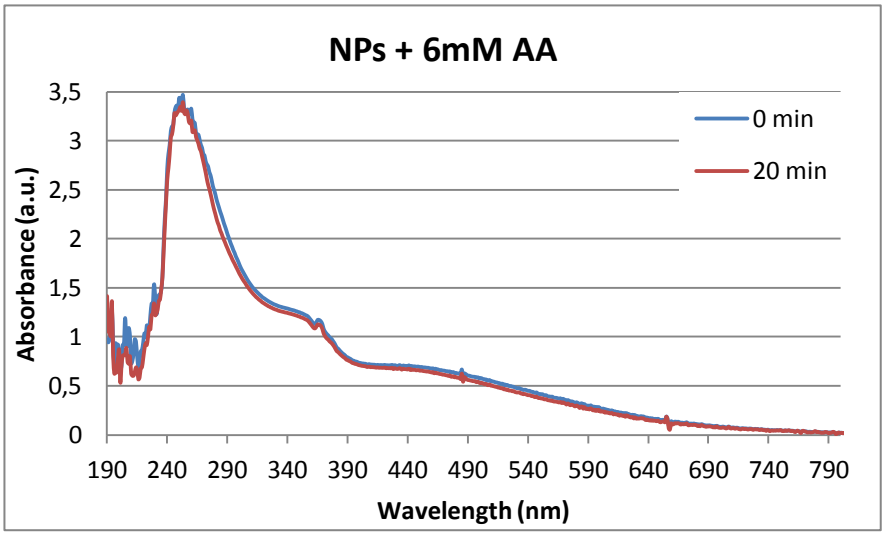
NPs + 6mM AA
Absorbance (a.u.)
3,5
3
2,5
2
1,5
1
0,5
0
190 240 290 340 390 440 490 540 590 640 690 740 790
Wavelength (nm)
0 min
20 min

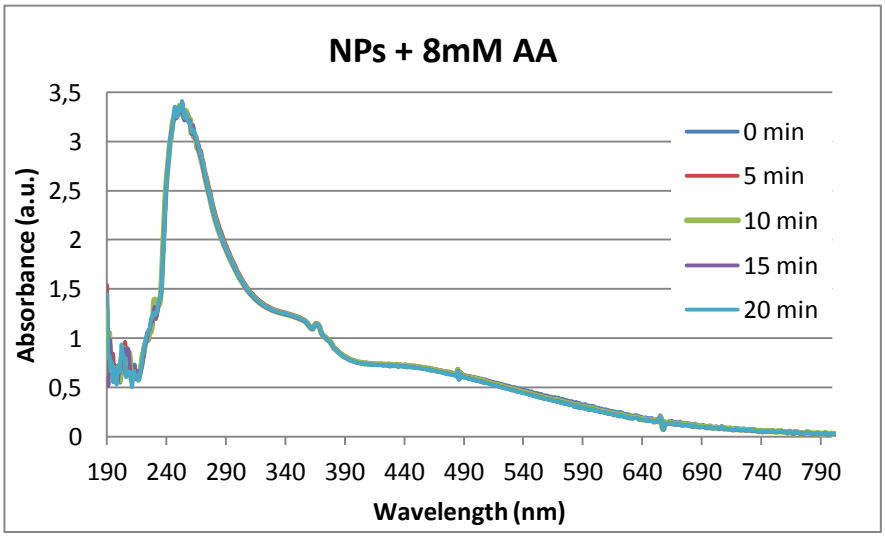
NPs + 8mM AA
Absorbance (a.u.)
3,5
3
2,5
2
1,5
1
0,5
0
190 240 290 340 390 440 490 540 590 640 690 740 790
Wavelength (nm)
0 min
5 min
10 min
15 min
20 min

A12 Results of peaks in nanoceria by catalytic reduction particle collision.

Some peaks obtained by direct modified PC following the general procedure and parameters collected in A7xi are shown.

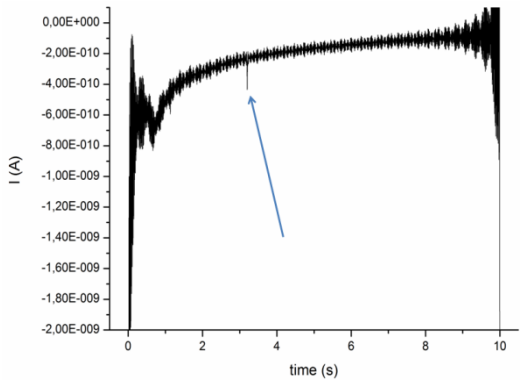

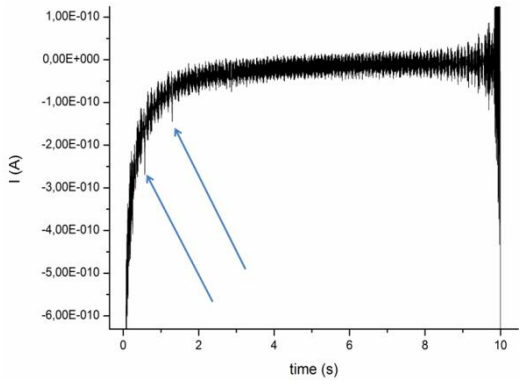

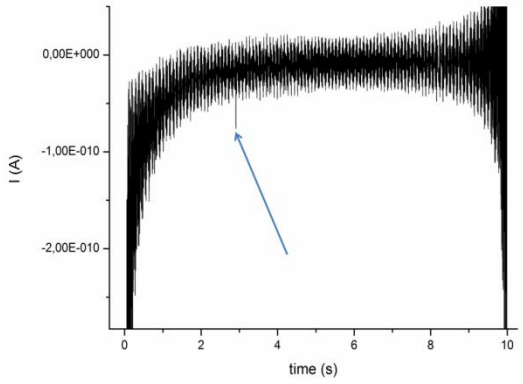

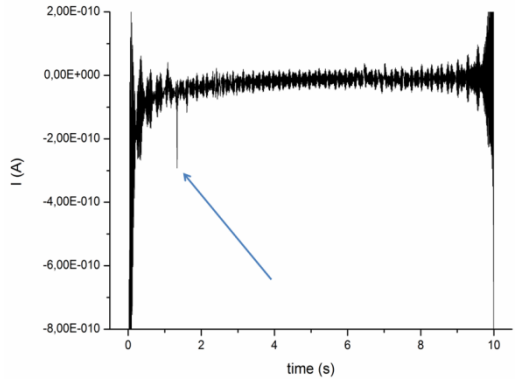

A13 Peaks in 10-20nm nanoceria by catalytic reduction particle collision.

Some peaks detected following the general procedure and parameters collected in A7xi are shown. Five graphics with peaks were superimposed in both plots.

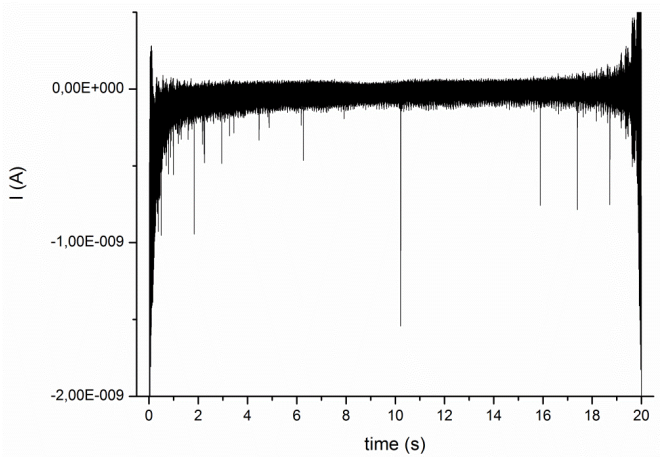

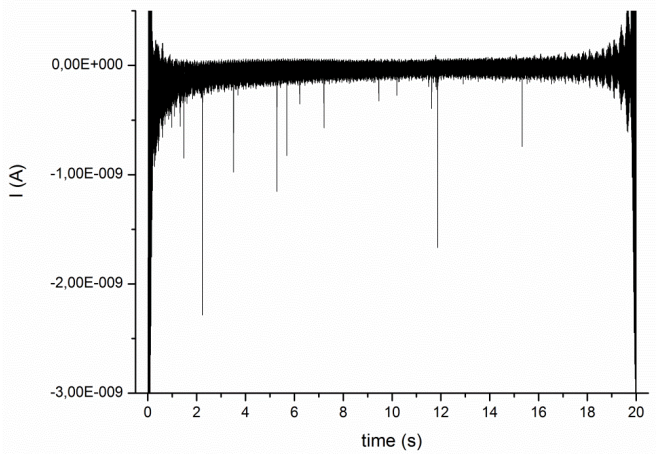

Peak oxidation obtained in this procedure and attributed to the oxidation of Ce^0.

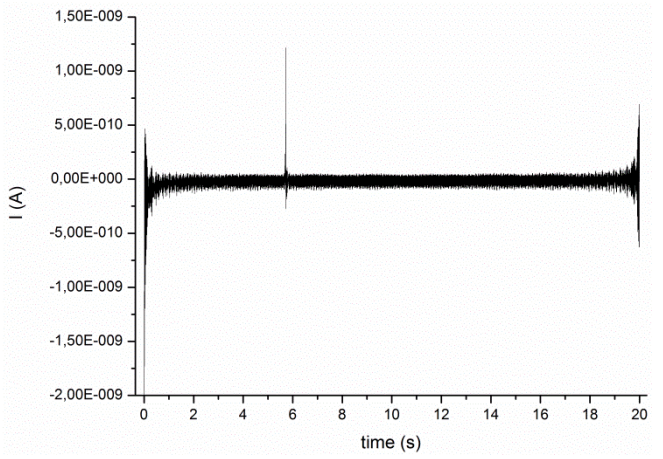

A14 TEM images and size distribution of 4nm nanoceria.

This annex has been written with permission and data provided by *Dra. Laura Sanchez.*

STEM equipment (Tecnai G2-F30 Field Emission Gun microscope) was working at 300kV with a super-twin lense and 0.2 nm point-to-point resolution and 0.1 line resolution. Nanoceria 4nm were prepared by depositing and air-drying a droplet on the carbon-coated 300 mesh copper grid. Images were obtained by GATAN CCD camera and subsequently analyzed with ImageJ 1.47 v. software. 100 NPs per image were analyzed in full five images.

Some STEM images and size distribution obtained from them are shown below in figures A14a and A14b respectively.

Figure A14a. STEM image of 4nm nanoceria.

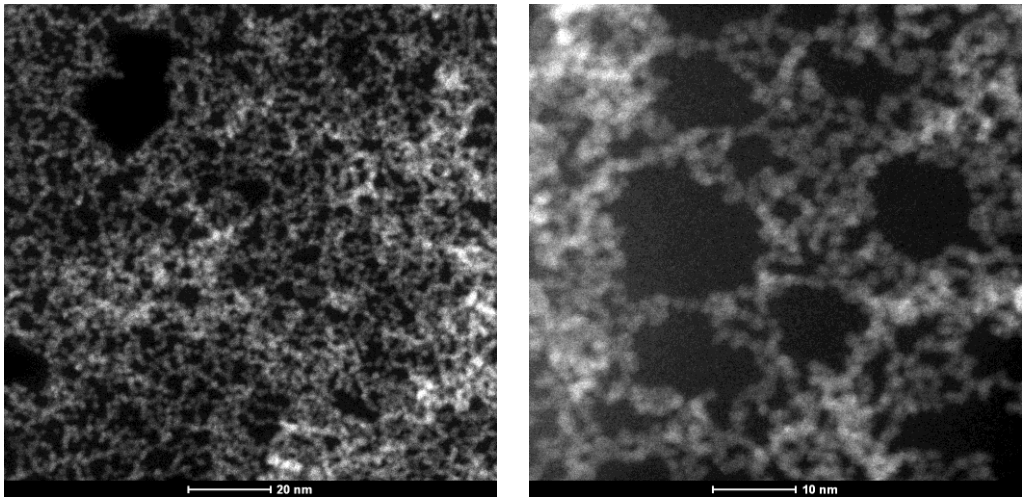

Figure A14b. Size distribution obtained from image analysis of 4nm nanoceria.

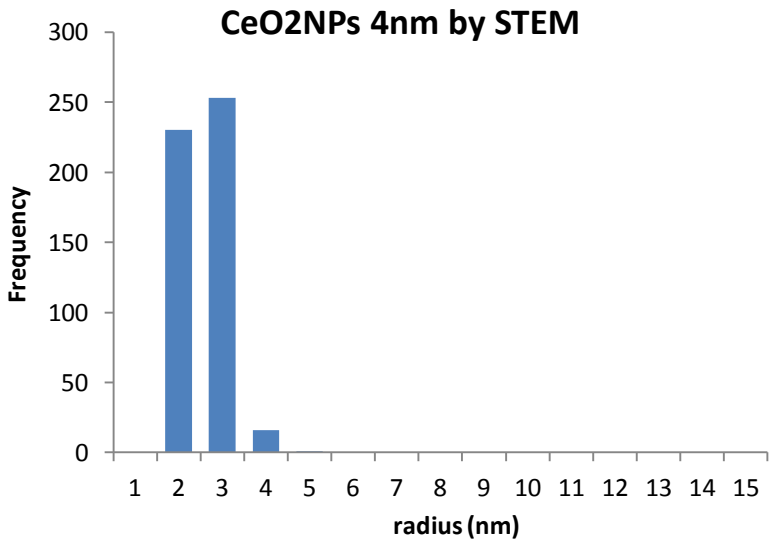

9. REFERENCES

[1] Marissa D. Newman et.al., "The safety of nanosized particles in titanium oxide and zinc oxide based sunscreen", *J. Am. Acad. Dermatol.*, 61, 4, **2009**, 685-692.

[2] Catalina Marambio-Jones & Eric M. V. Hoek, "A review of the antibacterial effects of silver nanomaterials and potential implications for human health and the environment", *J. Nanopart. Res.*, 12, **2010**, 1531-1551.

[3] http://www.nanotechproject.org/cpi/products/babolat-r-nstm-drive-tennis-racket/ (Last time checked: 25/08/2014)

[4] Junfeng Zhang et.al., "Impacts of a Nanosized Ceria Additive on Diesel Engine Emissions of Particulate and Gaseous Pollutants", *Environ. Sci. Technol.*, 47, **2013**, 13077-13085.

[5] http://www.nanotechproject.org/ (Last time checked: 20/08/2014)

[6] Daniel J. Fiorino, "Voluntary initiatives, regulation, and nanotechnology oversight: Charting a path", *PEN 19*, **November 2010**.

[7] Roya Dastjerdi & Majid Montazer, "A review on the application of inorganic nano-structured materials in the modification of textiles: Focus on anti-microbial properties", *Colloids and Surfaces B; Biointerfaces*, 79, **2010**, 5-18.

[8] Martin Hassellöv et. al., "Nanoparticle analysis and characterization methodologies in environmental risk assessment of engineered nanoparticles", *Ecotoxicology*, 17, **2008**, 344-361.

[9] Zong-ming Xiu et. al., "Negligible Particle-Specific Antibacterial Activity of Silver Nanoparticles", *Nano. Lett.*, 12, **2012**, 4271-4275.

[10] E. Bolea et. al., "Size characterization and quantification of silver nanoparticles by asymmetric flow field-flow fractionation coupled with inductively coupled plasma mass spectrometry", *Anal. Bioanal. Chem.*, 401, **2011**, 2723-2732.

[11] Vijay Ramani et. al., "CeO_2 Surface Oxygen Vacancy Concentration Governs in Situ free Radical Scavenging Efficacy in Polymer Electrolytes", *ACS Appl. Mater. Interfaces*, 4 (10), **2012**, 5098-5102.

[12] Eudald Casals & Victor Puntes, "La revolución del óxido de cerio. Nanopartículas de óxido de cerio: Un material multifuncional", *nano*, 1, No 1, **2013**. [www.revistanano.org]

[13] William T. Self et. al., "The role of cerium redox state in the SOD mimetic activity of nanoceria", *Biomaterials*, 29, **2008**, 2705-2709.

[14] Talib Pirmohamed et.al., "Nanoceria exhibit redox state-dependent catalase mimetic activity", *Chem. Commun.*, 46, **2010**, 2736-2738.

[15] William T. Self et. al., "A phosphate-dependent shift in redox state of cerium oxide nanoparticles and its effects on catalytic properties", *Biomaterials*, 32, **2011**, 6745-6753.

[16] James J. Hickman et. al., "Auto-catalytic ceria nanoparticles offer neuroprotection to adult rat spinal cord neurons", *Biomaterials*, 28, **2007**, 1918-1925.

[17] Francisca Fernández-Piñas et. al., "An insight into the mechanisms of nanoceria toxicity in aquatic photosynthetic organisms", *Aquatic Toxicology*, 122-123, **2012**, 133-143.

[18] Barbara K. Pierscionek et. al., "The effect of high concentration and exposure duration of nanoceria on human lens epithelial cells", *Nanomedicine: Nanotechnology, Biology, and Medicine*, 8, **2012**, 383-390.

[19] Robert A. Yokel et. al., "Biodistribution and biodispersistence of ceria engineered nanomaterials: size dependence", *Nanomedicine: Nanotechnology, Biology, and Medicine*, 9, **2013**, 398-407.

[20] Fritz Scholz & Birgit Lange, "Abrasive stripping voltammetry-an electrochemical solid state spectroscopy of wide applicability", *TrAC*, 11, **1992**, 359-367.

[21] Fritz Scholz & Birgit Meyer, "Electrochemical Solid State Analysis: State of the Art", *Chem. Soc. Rev.*, 23, **1994**, 341-347.

[22] Book: F. Scholz, U. Schröder, R. Gulaboski, "Electrochemistry of Inmobilized Particles and Droplets", Springer Science & Business Media, 290 pages.

[23] Fritz Scholz, "The electrochemistry of particles, droplets, and vesicles-the present situation and future tasks", *J. Solid State Electrochem.*, 15, **2011**, 1699-1702.

[24] Kh. Z. Brainina et. al., "Silver nanoparticles electrooxidation: theory and experiment", *J. Solid State Electrochem.*, 16, **2012**, 2365-2372.

[25] Kh. Z. Brainina et. al., "The effect of the system polydispersity on voltammograms of nanoparticles electrooxidation", *J. Solid State Electrochem.*, 17, **2013**, 43-53.

[26] Khiena. Z. Brainina et. al., "Mathematical modeling and numerical simulation of metal nanoparticles electrooxidation", *J. Solid State Electrochem.*, 14, **2010**, 981-988.

[27] G. Cepriá et. al., "Silver nanoparticle detection and characterization in silver colloidal products using screen printed electrodes", *Anal. Methods*, 6, **2014**, 3072-3078.

[28] Kh. Z. Brainina et. al., "Electrochemistry of metal nanoparticles: the effect of substrate", *J. Solid State Electrochem.*, 16, **2012**, 2357-2363.

[29] Book: "Nanomaterials. Chapter 1.1: Primary Particles-Agglomerates-Agregates", Dr. Dirk Walter, 2013. Wiley-VCH Verlag GmbH & Co.

[30] Justin M. Gorham et. al., "UV-induced photochemical transformations of citrate-capped silver nanoparticle suspensions", *J. Nanopart. Res.*, 14, **2012**, 1139.

[31] http://www.sigmaaldrich.com/materials-science/nanomaterials/silver-nanoparticles.html
(last time checked: 26/08/2014)

[32] http://www.bbisolutions.com/products/type/silver-nanoparticles
(last time checked: 26/08/2014)

[33] http://nanocomposix.eu/collections/silver/silver#collection-filters
(last time checked: 26/08/2014)

[34] M. Heyrovský & J. Jirkovský, "Polarography and Voltammetry of Ultrasmall Colloids: Introduction to a New Field", *Langmuir*, 11, **1995**, 4288-4292.

[35] M. Heyrovský & J. Jirkovský, "Polarography and Voltammetry of Aqueous Colloidal SnO_2 Solutions", *Langmuir*, 11, **1995**, 4293-4299.

[36] M. Heyrovský & J. Jirkovský, "Polarography and Voltammetry of Aqueous Colloidal TiO_2 Solutions", *Langmuir*, 11, **1995**, 4300-4308.

[37] M. Heyrovský & J. Jirkovský, "Polarography and Voltammetry of Mixed Titanium (IV) Oxide/Iron(III) Oxide Colloids", *Langmuir*, 11, **1995**, 4309-4312.

[38] Allen J. Bard et. al., "Current Transient in Single Nanoparticle Collision Events", *J. Am. Chem. Soc.*, 130, **2008**, 16669-16677.

[39] Allen J. Bard et. al., "Observing single Nanoparticle Collisions at an Ultramicroelectrode by Electrocatalytic Amplification", *J. Am. Chem. Soc.*, 129, **2007**, 9610-9612.

[40] Allen J. Bard et. al., "Observing Iridium Oxide (IrOx) Single Nanoparticle Collisions at Ultramicroelectrodes", *J. Am. Chem. Soc.*, 132, **2010**, 13165-13167.

[41] Allen J. Bard et. al., "Observing Single Nanoparticle Collisions by Electrogenerated Chemiluminescence Amplification", *Nano Lett.*, 8, **2008**, 1746-1749.

[42] G. Compton et. al., "Nanoparticle-electrode impacts: the oxidation of copper nanoparticles has slow kinetics", *Phys. Chem. Chem. Phys.*, 14, **2012**, 13612-13617.

[43] G. Compton et. al., "The Aggregation of silver Nanoparticles in Aqueous Solution Investigated via Anodic Particle Coulometry", *ChemPhysChem*, 12, **2011**, 1645-1647.

[44] G. Compton et. al., "Electrode-nanoparticle collisions: The measurement of the sticking coefficients of gold and nickel nanoparticles from aqueous solution onto a carbon electrode", *Chemical Physics Letters*, 551, **2012**, 68-71.

[45] G. Compton et. al., "Gold nanoparticles show electroactivity: counting and sorting nanoparticles upon impact with electrodes", *Chem. Commun.*, 48, **2012**, 224-226.

[46] G. Compton et. al., "Electrode-nanoparticles collision: The measurements of the sticking coefficient of silver nanoparticles on a glassy carbon electrode", *Chemical Physics Letters*, 514, **2011**, 291-293.

[47] Fritz Scholz et. al., "Detection of the adhesion events of dispersed single montmorillonite particles at a static mercury drop electrode", *Electrochemistry Communications*, 6, **2004**, 929-933.

[48] G. Compton et. al., "The non-destructive sizing of nanoparticles via particle-electrode collisions: Tag-redox coulometry (TRC)", *Chemical Physics Letters*, 525-526, **2012**, 69-71.

[49] G. Compton et. al., "Particle-impact voltammetry: The reduction of hydrogen peroxide at silver nanoparticles impacting a carbon electrode", *Chemical Physics Letters*, **531**, 2012, 94-97.

[50] Silvana Andreescu et. al., "Electroanalytical Evaluation of Antioxidant Activity of Cerium Oxide Nanoparticles by Nanoparticle Collisions at Microelectrodes", *J. Am. Chem. Soc.*, 135, **2013**, 16770-16773.

[51] José Mª Palacios-Santander et. a., "Study of the electrocatalytic activity of Cerium Oxide and Gold-studded cerium oxide nanoparticles using a sonogel-Carbon material as supporting electrode: Electroanalytical study in apple juice for babies", *Sensors*, 13, **2013**, 4979-5007.